

Towards the complete description of stationary states

# Towards the complete description of stationary states of a Bose-Einstein condensate in a one-dimensional quasiperiodic lattice: A coding approach

G. L. Alfimov<sup>\*,1</sup>, A. P. Fedotov,<sup>1</sup> Ya. A. Murenkov,<sup>1</sup> and D. A. Zezyulin<sup>2</sup>

<sup>1)</sup>*Moscow Institute of Electronic Engineering, Zelenograd, Moscow, 124498, Russia.*

<sup>2)</sup>*School of Physics and Engineering, ITMO University, St. Petersburg 197101, Russia*

(\*Electronic mail: galfimov@yahoo.com.)

(Dated: 20 February 2026)

We consider stationary states of an effectively one-dimensional Bose-Einstein condensate in a quasiperiodic lattice. We formulate sufficient conditions for a one-to-one correspondence between the stationary states with a fixed chemical potential and the set of bi-infinite sequences over a finite alphabet. These conditions can be checked numerically. A bi-infinite sequence can be interpreted as a code of the corresponding solution. A numerical example demonstrates the coding approach using an alphabet of three symbols.

**Quasiperiodic systems, characterized by the interplay between multiple incommensurate frequencies, represent a fundamental class of models in modern physics. They occupy an intermediate position between perfectly ordered periodic lattices and fully disordered systems, exhibiting a unique blend of properties from both extremes. The complex properties of quasiperiodic lattices are already apparent in the linear regime, where their spectra exhibit Anderson localization, mobility edges, and fractal structure. The interplay between quasiperiodicity and nonlinearity introduces an additional layer of complexity. Atomic Bose-Einstein condensates (BECs) represent a perfect platform, where the combination of both effects can be reached experimentally. Within the mean-field approximation, the stationary states of a BEC are described by the Gross-Pitaevskii equation (GPE). In the GPE with a periodic potential, each stationary state has a countable infinity of exact translational copies. This is not the case for quasiperiodic lattices, which lack translational symmetry; hence, each stationary state becomes unique. It may therefore seem unlikely that the full set of stationary states in a quasiperiodic potential admits a complete, unified description. In this paper we demonstrate that, in some cases, the stationary states emerging in a quasiperiodic lattice can be classified via a coding approach that establishes a one-to-one correspondence with the set of bi-infinite sequences over a specific alphabet. Our approach adapts a method originally developed for periodic lattices. The core idea is to filter out physically irrelevant singular solutions. The remaining regular solutions form a scarce set which can, in some cases, be completely described using symbolic dynamics. We extend this approach to the quasiperiodic setting and demonstrate that for a specific range of governing parameters the stationary states can be encoded by bi-infinite sequences of symbols from a finite alphabet.**

## I. INTRODUCTION

The interplay between incommensurate lattices is fundamental to the theory of quasicrystals<sup>1,2</sup>, with wide applications

in solid-state physics<sup>3,4</sup>, photonics<sup>5–8</sup>, and the study of atomic Bose-Einstein condensates<sup>9–14</sup>. Quasiperiodic systems can be regarded as intermediate between periodically ordered and fully disordered systems, retaining certain features of both. In particular, one-dimensional quasiperiodic lattices can exhibit Anderson localization<sup>15–18</sup> and have mobility edges in the energy spectra<sup>19–22</sup>, which separate spatially localized and extended states. On the other hand, spectra of quasiperiodic systems can sometimes be described in terms of generalized Bloch functions<sup>23,24</sup>, a concept typically associated with periodic systems.

The challenges posed by quasiperiodic systems are clearly evident even in the linear regime, as exemplified by the spectrum of the one-dimensional Schrödinger operator  $L = -\frac{d^2}{dx^2} + V(x)$ . If the potential  $V(x)$  is periodic, the band-gap structure of the spectrum follows from the Bloch theorem (1929). However, the spectrum becomes much more complex for a quasiperiodic potential  $V(x)$ <sup>25–31</sup>. Even for the prototypical bichromatic potential

$$V(x) = A_1 \cos(2x) + A_2 \cos(2\theta x + \delta),$$

where irrational  $\theta$  and real  $\delta \in [0, 2\pi)$  are fixed numbers, the lower spectral region typically contains discrete eigenvalues with localized eigenfunctions, while the overall structure of the spectrum depends on the parameters of the potential and is, generically, fractal<sup>21</sup>.

It is then natural to expect that the interplay between quasiperiodicity and nonlinearity leads to a further escalation in complexity. Bose-Einstein condensates (BECs) provide an ideal platform for probing this regime experimentally. Localization of a BEC arises from the interplay between the mean-field nonlinearity and the optical lattice potential generated by multiple laser sources<sup>32</sup>. If the lattice is periodic, the localized excitations appear at chemical potentials in the spectral gaps (the so-called *gap solitons*)<sup>33–38</sup>. Quasiperiodic optical lattices have been created in several experiments by superimposing standing waves with incommensurate wavelengths<sup>9–13</sup>. In parallel, the theoretical studies predict rich and complex behavior for nonlinear modes in one-dimensional quasiperiodic potentials<sup>39–45</sup>.

Apart from the trap potentials, the localization of BEC may be facilitated by nonlinear-lattice pseudopotentials cor-

responding to a spatially periodic modulation of the coefficient in front of the nonlinear term in the respective Gross-Pitaevskii equation<sup>46</sup>. This structure can be created in a BEC by means of the Feshbach resonance controlled by magnetic or optical fields<sup>47,48</sup>. Even when both the trap potential and pseudopotential are periodic, their frequencies may be incommensurate<sup>49,50</sup>, rendering the overall problem quasiperiodic.

Within the mean-field approximation, the dynamics of a cigar-shaped BEC are described by the Gross-Pitaevskii equation. In its dimensionless form, this equation is:

$$i\Psi_t = -\Psi_{xx} + V(x)\Psi + P(x)|\Psi|^2\Psi. \quad (1)$$

Here  $\Psi(t, x)$  is the macroscopic wavefunction,  $V(x)$  is the trap potential, and  $P(x)$  is the pseudopotential. Stationary states of the BEC correspond to solutions of the form

$$\Psi(t, x) = e^{-i\mu t}u(x), \quad (2)$$

where  $\mu$  is the chemical potential, and  $u(x)$  is the stationary wavefunction. In this paper, we assume that  $u(x)$  is real-valued. This assumption does not lead to a loss of generality if  $u(x)$  is a solitary wave which tends to zero  $x \rightarrow \infty$  and  $x \rightarrow -\infty$ . At the same time, our analysis is also applicable to real-valued stationary solutions that do not satisfy zero boundary conditions at  $x \rightarrow \pm\infty$ . The stationary wavefunction  $u(x)$  solves the equation

$$u_{xx} + (\mu - V(x))u + P(x)u^3 = 0. \quad (3)$$

In periodic lattices, every stationary state has a countable set of exact replicas that are equivalent under a translation. This is not the case for quasiperiodic lattices, which lack translational symmetry; hence, each stationary state is unique. It may therefore seem unlikely that the full set of stationary states in a periodic potential admits a complete, unified description. The main goal of this paper is to demonstrate that, in some cases, the real-valued stationary states emerging in a quasiperiodic lattice can be fully classified via a transparent coding procedure that establishes a one-to-one correspondence with the set of bi-infinite sequences over a specific alphabet. Our approach represents a deep extension of a method originally developed for the periodic version of Eq. (3), where  $V(x)$  and  $P(x)$  were periodic functions with a common period  $\ell$ <sup>51-56</sup>. The original method used the fact that for a sign-alternating or negative  $P(x)$  most solutions of the Cauchy problem for Eq. (3) tend to infinity at some finite point on the real axis<sup>57</sup>. We refer to such solutions as *singular*. These singular solutions are physically irrelevant. The remaining *regular* solutions form a scarce set which in some cases can be fully described using symbolic dynamics. When  $V(x)$  and  $P(x)$  are periodic with a common period  $\ell$ , one can analyze Eq. (3) using the Poincaré map, defined as follows:

$$\mathcal{P} \begin{pmatrix} u_0 \\ u'_0 \end{pmatrix} = \begin{pmatrix} u_\ell \\ u'_\ell \end{pmatrix}. \quad (4)$$

Here  $u_\ell = u(\ell)$ ,  $u'_\ell = u_x(\ell)$ , and  $u(x)$  is a solution of the Cauchy problem for Eq. (3) with the initial conditions  $u(0) =$

$u_0$ ,  $u_x(0) = u'_0$ . Due to the presence of singular solutions, the Poincaré map is defined not on the whole plane of initial data  $(u, u')$  but on some domain  $\mathcal{U}_\ell^+ \subset \mathbb{R}^2$ . If the action of  $\mathcal{P}$  on  $\mathcal{U}_\ell^+$  is hyperbolic and conjugate to a Smale horseshoe map, then the regular solutions can be described, either completely or partially, by bi-infinite sequences of symbols (also called codes) from a finite alphabet<sup>55,56</sup>. Verifying the hyperbolic properties of the map  $\mathcal{P}$  requires checking the hypotheses formulated in Ref.<sup>56</sup>, either numerically or analytically.

This approach cannot be applied directly if  $V(x)$  or  $P(x)$  is quasiperiodic, or if both are periodic with incommensurate periods. In the present study we develop an extension of this method to the quasiperiodic case. The extended approach covers various important prototypical cases, as follows

$$(a) V(x) = A_1 \cos x + A_2 \cos(\theta x + \delta), \quad P(x) = -1, \quad (5)$$

$$(b) V(x) = A_1 \cos x, \quad P(x) = -1 + A_2 \cos(\theta x + \delta), \quad (6)$$

$$(c) V(x) = 0, \quad P(x) = -1 + A_1 \cos x + A_2 \cos(\theta x + \delta), \quad (7)$$

where  $A_{1,2}$  are real amplitudes,  $0 \leq \delta < 2\pi$  and  $\theta > 1$  is an irrational number.

The paper is organized as follows. Section II introduces the main concepts and basic definitions used throughout the paper. In Sec. III we formulate two conditions that guarantee the existence of a one-to-one correspondence between regular solutions of quasiperiodic Eq. (3) and bi-infinite sequences over some alphabet. Direct verification of these conditions, however, is challenging. Therefore, in Sec. IV, we formulate two theorems that render these conditions amenable to a numerical check. In Sec. VI we apply our approach to Eq. (3) with quasiperiodic potential  $V(x)$  with  $P(x) \equiv -1$  (the case (a), Eq. (5)). Section VIII provides a summary and discussion.

## II. THE BASIC EQUATION AND DEFINITIONS

### A. The basic equation

In this study, we focus on the equation

$$\ddot{u} = G_\delta(x, u), \quad (8)$$

where  $\ddot{u}$  is the second derivative with respect to  $x$ ,

$$G_\delta(x, u) = F(x, \theta x + \delta, u), \quad \theta > 1, \quad (9)$$

and  $0 \leq \delta < 2\pi$  is a fixed given parameter. It is assumed that the function  $F(X, Y, u)$  satisfies the following conditions:

- (A)  $F(X, Y, u) \in C^1(\mathbb{R}^3)$ ;
- (B)  $F(X, Y, 0) = 0$  for any  $X, Y \in \mathbb{R}$ ;
- (C)  $F(X, Y, u)$  is  $2\pi$ -periodic with respect to both  $X$  and  $Y$ .

If  $\theta$  is a rational number, the right-hand side of Eq. (8) is periodic with respect to  $x$ . Without loss of generality, it can be assumed that the period is equal to  $2\pi$  (this can

be achieved by renormalizing the independent variable and rescaling the function  $F(X, Y, u)$  itself). Equation (3) with (pseudo)potentials given by either (5) or (6) can be cast in the form (8) if we assume

- (a)  $F(X, Y, u) = -(\mu - A_1 \cos X - A_2 \cos Y)u + u^3,$
- (b)  $F(X, Y, u) = -(\mu - A_1 \cos X)u + (1 - A_2 \cos Y)u^3,$
- (c)  $F(X, Y, u) = -\mu u + (1 - A_1 \cos X - A_2 \cos Y)u^3.$

## B. The space $\mathbb{S}^1$ and the auxiliary family of equations

The quotient space  $\mathbb{S}^1 = \mathbb{R}/2\pi\mathbb{Z}$  is a set of real numbers, where any two points  $x, y$  are considered equivalent if their difference is an integer multiple of  $2\pi$ , i.e.,  $x \sim y$  iff  $x - y = 2\pi n, n \in \mathbb{Z}$ . If  $\Delta \in \mathbb{S}^1$ , then without loss of generality it can be assumed that  $\Delta \in [0, 2\pi)$ . From the geometric point of view,  $\mathbb{S}^1$  can be identified with the unit circle parameterized by the rotation angle  $\Delta$ . The sum (to be denoted as  $\oplus$ ) and difference ( $\ominus$ ) of any two elements from  $\mathbb{S}^1$  will be computed modulo  $2\pi$ . Using the argument function from the complex analysis, for any  $\Delta_{1,2} \in \mathbb{S}^1$  these operations can be defined as

$$\Delta_1 \oplus \Delta_2 = \text{Arg} e^{i(\Delta_1 + \Delta_2)}, \quad \Delta_1 \ominus \Delta_2 = \text{Arg} e^{i(\Delta_1 - \Delta_2)}, \quad (10)$$

where  $+$  and  $-$  denote the usual sum and difference in  $\mathbb{R}$ ,  $i$  is the imaginary unit,  $\text{Arg}$  is the principal value of the argument, and we use the convention where  $\text{Arg} z \in [0, 2\pi)$ .

Equation (8) is a representative of a family of equations

$$\ddot{u} = G_\Delta(x, u), \quad G_\Delta(x, u) = F(x, \theta x + \Delta, u), \quad (11)$$

parametrized by  $\Delta \in \mathbb{S}^1$ .

## C. Regular and singular solutions

**Definition 1** A solution  $u(x)$  of Eq. (11) is called *singular* on an interval  $[a, b]$  if it tends to infinity at some finite point  $x_c \in [a, b]$  approaching  $x_c$  from the left, from the right or from both sides, i.e.,

$$\lim_{x \rightarrow x_c^-} |u(x)| = \infty \quad \text{or} \quad \lim_{x \rightarrow x_c^+} |u(x)| = \infty.$$

Alternatively, we say that  $u(x)$  *collapses* at  $x = x_c$ .

**Definition 2** A solution is called *regular* on  $[a, b]$  if it is not singular on  $[a, b]$ . A solution is called *regular on  $\mathbb{R}$*  if it is not singular on  $[a, b]$  for any  $a$  and  $b$  such that  $-\infty < a < b < \infty$ .

Singular solutions are abundant for Eq. (11). Indeed, singular solutions are known to exist<sup>57</sup> for Eq. (3) with the (pseudo)potentials (5) and (6). The following proposition provides sufficient conditions for the existence of singular solutions for Eq. (3).

**Proposition 1** Let  $\Omega$  be a small enough neighbourhood of a point  $x_c$ , such that  $P(x_c) < 0$  and  $V(x) \in C^2(\Omega)$ ,  $P(x) \in C^4(\Omega)$ .

Then there exist two  $C^1$ -smooth one-parametric families of solutions for equation (3) that are defined in  $\Omega$  and collapsing at the point  $x = x_c$  while approaching from the left,  $x < x_c$ . These two families are connected by the symmetry  $u \rightarrow -u$ . Each of these families can be parametrized by a free variable  $C \in \mathbb{R}$ .

Proposition 1 does not assume periodicity or quasiperiodicity of  $V(x)$  and  $P(x)$ .

## D. The map $\mathcal{P}$

Consider  $\mathcal{L} = \mathbb{S}^1 \times \mathbb{R}^2$ , the space of all triples  $(\Delta, u, u')$  with  $\Delta \in \mathbb{S}^1$  and  $(u, u') \in \mathbb{R}^2$ .

The map  $\mathcal{P}: \mathcal{L} \rightarrow \mathcal{L}$  is defined as follows:  $\mathcal{P}(\mathbf{p}_0) = \mathbf{p}_1$ , where  $\mathbf{p}_0 = (\Delta_0, u_0, u'_0)$ ,  $\mathbf{p}_1 = (\Delta_1, u_1, u'_1)$ , and

- $\Delta_1 = \Delta_0 \oplus 2\theta\pi;$
- $u_1 = u(2\pi)$ ,  $u'_1 = \dot{u}(2\pi)$  where  $u(x)$  is the solution of the Cauchy problem for Eq. (11) with  $\Delta = \Delta_0$  and the initial conditions  $u(0) = u_0$ ,  $\dot{u}(0) = u'_0$ .

The inverse map  $\mathcal{P}^{-1}: \mathcal{L} \rightarrow \mathcal{L}$  acts as follows:

$$\mathcal{P}^{-1}(\mathbf{p}_0) = \mathbf{p}_{-1},$$

where  $\mathbf{p}_0 = (\Delta_0, u_0, u'_0)$ ,  $\mathbf{p}_{-1} = (\Delta_{-1}, u_{-1}, u'_{-1})$ ,  $\Delta_{-1} = \Delta_0 \ominus 2\theta\pi$ ,  $u_{-1} = u(-2\pi)$ ,  $u'_{-1} = \dot{u}(-2\pi)$ , and  $u(x)$  is the solution of the Cauchy problem for Eq. (11) with  $\Delta = \Delta_0$  and the initial conditions  $u(0) = u_0$ ,  $\dot{u}(0) = u'_0$ .

**Definition 3** We call  $\Delta$ -slice the plane  $\mathcal{L}_\Delta \subset \mathcal{L}$  for a fixed  $\Delta$ ,  $\mathcal{L}_\Delta = \mathcal{L}|_\Delta$ .

**Remark** It follows from the definition of  $\mathcal{P}$  that its restriction from  $\mathcal{L}$  to  $\mathcal{L}_\Delta$  acts to  $\mathcal{L}_{\Delta \oplus 2\theta\pi}$ , and the restriction of  $\mathcal{P}^{-1}$  to  $\mathcal{L}_\Delta$  acts to  $\mathcal{L}_{\Delta \ominus 2\theta\pi}$ , i.e.,

$$\mathcal{P}|_{\mathcal{L}_\Delta}: \mathcal{L}_\Delta \rightarrow \mathcal{L}_{\Delta \oplus 2\theta\pi}, \quad \mathcal{P}^{-1}|_{\mathcal{L}_\Delta}: \mathcal{L}_\Delta \rightarrow \mathcal{L}_{\Delta \ominus 2\theta\pi}.$$

**Definition 4** An orbit is a sequence of points  $\{\mathbf{p}_n\}$ ,  $\mathbf{p}_n \in \mathcal{L}$ , such that  $\mathcal{P}(\mathbf{p}_n) = \mathbf{p}_{n+1}$ ,  $n = 0, \pm 1, \dots$

Since Eq. (11) may have singular solutions, the maps  $\mathcal{P}$  and  $\mathcal{P}^{-1}$  may not be defined in the whole  $\mathcal{L}$ . Consequently, the iterations of  $\mathcal{P}$  or  $\mathcal{P}^{-1}$  may stop after a finite number of steps. Therefore, an orbit  $\{\mathbf{p}_n\}$  is not necessarily bi-infinite. The following statement establishes a natural correspondence between the bi-infinite orbits of  $\mathcal{P}$  and the regular solutions of Eq. (8).

**Lemma 1** The solution  $u(x)$  of the Cauchy problem for Eq. (8) with initial data  $u(0) = u_0$ ,  $\dot{u}(0) = u'_0$  is regular on  $\mathbb{R}$  iff the orbit  $\{\mathbf{p}_n\}$  generated by  $\mathcal{P}$  with  $\mathbf{p}_0 = (\delta, u_0, u'_0)$  is bi-infinite. The regular solution  $u(x)$  and the orbit  $\{\mathbf{p}_n\}$  are related as

$$\mathbf{p}_n = (\delta \oplus 2n\theta\pi, u(2n\pi), \dot{u}(2n\pi)), \quad n \in \mathbb{Z}.$$

**Proof** Let the solution  $u(x)$  of Eq. (8) with  $u(0) = u_0$ ,  $\dot{u}(0) = u'_0$  exist on  $[0; 2\pi]$ . This is equivalent to the map  $\mathcal{P}$  being defined at  $\mathbf{p}_0 = (\delta, u_0, u'_0)$  and, by definition of  $\mathcal{P}$ , we have  $\mathcal{P}(\mathbf{p}_0) = \mathbf{p}_1 = (\Delta_1, u(2\pi), u'(2\pi))$ , where  $\Delta_1 = \delta \oplus 2\theta\pi$ .

Let, in addition, the same solution  $u(x)$  exist on  $[2\pi, 4\pi]$ . Due to  $2\pi$ -periodicity of  $F(X, Y, u)$  in  $X$  and  $Y$ , this is equivalent to  $\mathcal{P}$  being defined at  $\mathbf{p}_1$ , and by definition of  $\mathcal{P}$ , we have  $\mathcal{P}(\mathbf{p}_1) = \mathbf{p}_2 = (\Delta_2, u(4\pi), u'(4\pi))$ , where  $\Delta_2 = \Delta_1 \oplus 2\theta\pi$ . Using the definition of  $\oplus$  in Eq. (10), it is easy to establish that  $\Delta_2 = \delta \oplus 4\theta\pi$ .

Repeating the procedure, we show that the existence of  $u(x)$  on the semi-axis  $x \geq 0$  is equivalent to the existence of the infinite sequence  $\mathbf{p}_0, \mathbf{p}_1, \mathbf{p}_2, \dots, \mathbf{p}_{n+1} = \mathcal{P}(\mathbf{p}_n)$ . Similarly,  $u(x)$  exists on the semi-axis  $x \leq 0$  iff there exists the backward-infinite sequence  $\mathbf{p}_0, \mathbf{p}_{-1}, \mathbf{p}_{-2}, \dots$ , where  $\mathbf{p}_{n-1} = \mathcal{P}^{-1}(\mathbf{p}_n)$ .  $\square$

Let us introduce several additional notations. Let  $\mathcal{U}^+ \subset \mathcal{L}$  be the domain of  $\mathcal{P}$ , and let  $\mathcal{U}^- \subset \mathcal{L}$  be the domain of  $\mathcal{P}^{-1}$ . Introduce

$$\mathcal{U} = \mathcal{U}^+ \cap \mathcal{U}^-.$$

For a fixed  $\Delta_0 \in \mathbb{S}^1$  we denote  $\mathcal{U}_{\Delta_0}^+ = \mathcal{U}^+ \cap \mathcal{L}_{\Delta_0}$ ,  $\mathcal{U}_{\Delta_0}^- = \mathcal{U}^- \cap \mathcal{L}_{\Delta_0}$  and

$$\mathcal{U}_{\Delta_0} = \mathcal{U}_{\Delta_0}^+ \cap \mathcal{U}_{\Delta_0}^-.$$

**Remark** The following comments are in order.

- (i) Note that  $\mathbf{p}_0 = (\Delta_0, u_0, u'_0) \notin \mathcal{U}^+$  iff the solution of the Cauchy problem for the equation  $\ddot{u} = G_{\Delta_0}(x, u)$  with the initial data  $u(0) = u_0$ ,  $\dot{u}(0) = u'_0$  collapses at some point  $x = x_0 \in (0, 2\pi]$ . Similarly,  $\mathbf{p}_0 = (\Delta_0, u_0, u'_0) \notin \mathcal{U}^-$  iff the solution of the same Cauchy problem collapses at some point  $x = x_0 \in [-2\pi, 0)$ .
- (ii) If  $\theta = 1$  then  $\mathcal{P}(\mathcal{U}_{\Delta_0}^+) \subset \mathcal{L}_{\Delta_0}$ ,  $\mathcal{P}^{-1}(\mathcal{U}_{\Delta_0}^-) \subset \mathcal{L}_{\Delta_0}$ , for any  $\Delta_0 \in \mathbb{S}^1$ .
- (iii) For any  $\theta$  and  $\Delta_0 \in \mathbb{S}^1$  the following relations hold:

$$\mathcal{P}(\mathcal{U}_{\Delta_0}^+) = \mathcal{U}_{\Delta_0 \oplus 2\theta\pi}^-, \quad \mathcal{P}^{-1}(\mathcal{U}_{\Delta_0}^-) = \mathcal{U}_{\Delta_0 \oplus 2\theta\pi}^+.$$

## E. Islands, Donuts, Curves and Strips

**Definition 5** Let  $\gamma > 0$  be fixed. A function  $f(x): [a, b] \rightarrow \mathbb{R}$  is called  $\gamma$ -Lipschitz function if for any  $x_1, x_2 \in [a, b]$  the inequality holds:

$$|f(x_1) - f(x_2)| \leq \gamma |x_1 - x_2|. \quad (12)$$

**Remark** Evidently, if a function is a  $\gamma_1$ -Lipschitz function and  $\gamma_2 > \gamma_1$  then  $f(x)$  is also  $\gamma_2$ -Lipschitz function.

**Remark** The union of  $\gamma$ -Lipschitz functions on  $[a; b]$  for  $\gamma \in [0; +\infty)$  constitutes the Banach space  $\text{Lip}(a; b)$  with respect to the norm<sup>58</sup>

$$\|f(x)\|_{\text{Lip}} = \sup_{x \in [a; b]} |f(x)| + \sup_{x, y \in [a; b], x \neq y} \frac{|f(x) - f(y)|}{|x - y|}.$$

If a sequence  $\{f_n(x)\}$  of  $\gamma$ -Lipschitz functions converges in  $\text{Lip}(a; b)$  to  $f(x)$  then  $f(x)$  is also a  $\gamma$ -Lipschitz function.

We call function  $f(x)$  monotonically increasing if for  $x_1 < x_2$ ,  $f(x_1) \leq f(x_2)$ , and monotonically decreasing if  $f(x_1) \geq f(x_2)$ , i.e. the inequalities are not strict. We also say that for functions  $f(x)$  and  $g(x)$  the type of monotonicity coincides or  $f(x)$  and  $g(x)$  are of the same type of monotonicity if both  $f(x)$  and  $g(x)$  are increasing or both  $f(x)$  and  $g(x)$  are decreasing functions simultaneously.

**Definition 6** A  $\gamma$ -island is an open curvilinear quadrangle  $D_\Delta \subset \mathcal{L}_\Delta$  formed by two pairs of curves  $\alpha^\pm, \beta^\pm$ , such that:

- curves  $\alpha^\pm$  do not intersect, they are graphs of monotonic  $\gamma$ -Lipschitz functions  $u' = h_\pm(u)$  of the same type of monotonicity, and any solution of equation (11) with initial conditions  $u(0) = u_0$ ,  $\dot{u}(0) = u'_0$  such that  $(u_0, u'_0) \in \alpha^\pm$  collapses at the point  $x = -2\pi$ ;
- curves  $\beta^\pm$  do not intersect, are graphs of monotonic  $\gamma$ -Lipschitz functions  $u = v_\pm(u')$  of the same type of monotonicity, and any solution of equation (11) with initial conditions  $u(0) = u_0$ ,  $\dot{u}(0) = u'_0$  such that  $(u_0, u'_0) \in \beta^\pm$  collapses at the point  $x = 2\pi$ ;
- if the functions  $h^\pm(u)$  are increasing then  $v^\pm(u')$  are decreasing, and vice versa, if functions  $h^\pm(u)$  are decreasing then  $v^\pm(u')$  are increasing respectively.

**Remark** When defining  $\gamma$ -island we keep in mind the following. Let  $\alpha^\pm$  be graphs of  $\gamma_\alpha^\pm$ -Lipschitz functions  $u' = h_\pm(u)$  and  $\beta^\pm$  be graphs of  $\gamma_\beta^\pm$ -Lipschitz functions  $u = v_\pm(u')$ . Taking

$$\gamma = \max(\gamma_\alpha^-, \gamma_\alpha^+, \gamma_\beta^-, \gamma_\beta^+)$$

one has that  $u' = h_\pm(u)$  and  $u = v_\pm(u')$  are  $\gamma$ -Lipschitz functions and they bound  $\gamma$ -island in the sense of Definition 6.

**Remark** If  $D_\Delta$  is a  $\gamma_1$ -island and  $\gamma_2 > \gamma_1$  then  $D_\Delta$  also is a  $\gamma_2$ -island.

**Remark** The  $\gamma$ -islands situated in  $\mathcal{L}_\Delta$  can be regarded as connected components of the set  $\mathcal{U}_\Delta$ . At the same time we do not claim that in generic situation the set  $\mathcal{U}_\Delta$  is composed by  $\gamma$ -islands only.

**Remark** The map  $\mathcal{P}$  sends the island  $D_\Delta \subset \mathcal{U}_\Delta \subset \mathcal{L}_\Delta$  to  $\mathcal{L}_{\Delta_1}$  where  $\Delta_1 = \Delta \oplus 2\theta\pi$ . Similarly,  $\mathcal{P}^{-1}$  maps  $D_\Delta$  to  $\mathcal{L}_{\Delta_{-1}}$  where  $\Delta_{-1} = \Delta \ominus 2\theta\pi$ . The points at the boundaries  $\beta^\pm$  of  $D_\Delta$  are mapped by  $\mathcal{P}$  to infinity at  $\mathcal{L}_{\Delta_1}$ . The points at  $\alpha^\pm$  are mapped by  $\mathcal{P}^{-1}$  to infinity at  $\mathcal{L}_{\Delta_{-1}}$ .

**Definition 7** Let  $D_\Delta \subset \mathcal{L}_\Delta$  be a  $\gamma$ -island bounded by curves  $\alpha^\pm, \beta^\pm$ . Let a curve  $\alpha$  connect the opposite sides  $\beta^\pm$  of the island  $D_\Delta$ .

- We say that  $\alpha$  is  $h_\gamma$ -curve if it is a graph of a monotonic  $\gamma$ -Lipschitz function  $u' = h(u)$  and its type of monotonicity coincides with the functions  $u' = h_\pm(u)$  that correspond to the  $\alpha^\pm$  boundaries of the island  $D_\Delta$ .

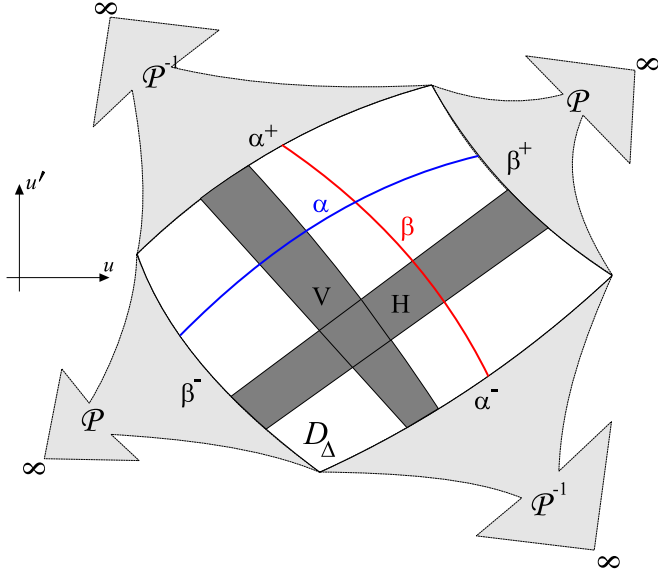


FIG. 1. An island  $D_\Delta$  bounded by curves  $\alpha^\pm, \beta^\pm$ ;  $h$ -curve  $\alpha$ ,  $v$ -curve  $\beta$ , and two strips:  $h$ -strip  $H$  and  $v$ -strip  $V$ .

- We say that  $\alpha$  is increasing/decreasing if it is a graph of *increasing/decreasing* function  $u' = f(u)$ .

**Definition 8** We call  $h_\gamma$ -strip an open subset of  $\gamma$ -island  $D_\Delta$  bounded by two  $h_\gamma$ -curves.

**Definition 9** Let  $D_\Delta \subset \mathcal{L}_\Delta$  be a  $\gamma$ -island bounded by curves  $\alpha^\pm, \beta^\pm$ . Let a curve  $\beta$  connect the opposite sides  $\alpha^\pm$  of island  $D_\Delta$ .

- We say that  $\beta$  is  $v_\gamma$ -curve if it is a graph of a monotonic  $\gamma$ -Lipschitz function  $u = v(u')$  and its type of monotonicity coincides with the functions  $u = v_\pm(u')$  that correspond to the  $\beta^\pm$  boundaries of the  $\gamma$ -island  $D_\Delta$ .
- We say that  $\beta$  is increasing / decreasing if  $\beta$  is a graph of increasing / decreasing function  $u = f(u')$ .

**Definition 10** We call  $v_\gamma$ -strip an open subset of  $\gamma$ -island  $D_\Delta$  bounded by two  $v_\gamma$ -curves.

**Remark** A  $\gamma$ -island is both  $h_\gamma$ -strip and  $v_\gamma$ -strip.

**Remark** It is important that the type of strip ( $h_\gamma$ -strip or  $v_\gamma$ -strip) is defined *not* by the type of monotonicity of its borders (increasing or decreasing) but the type of boundaries that it connects ( $\alpha^\pm$  or  $\beta^\pm$ ).

Figure 1 illustrates the definitions of a  $\gamma$ -island,  $h$ -curve,  $v$ -curve,  $h$ -strip, and  $v$ -strip.

**Definition 11** Assume that

- for any  $\Delta \in \mathbb{S}^1$  there exists a  $\gamma$ -island  $D_\Delta \subseteq \mathcal{U}_\Delta$ ;
- when  $\Delta \in \mathbb{S}^1$  varies, the  $\gamma$ -island  $D_\Delta$  undergoes a continuous deformation in such a way that its boundaries  $\alpha_\Delta^\pm$  and  $\beta_\Delta^\pm$  conserve the type of monotonicity.

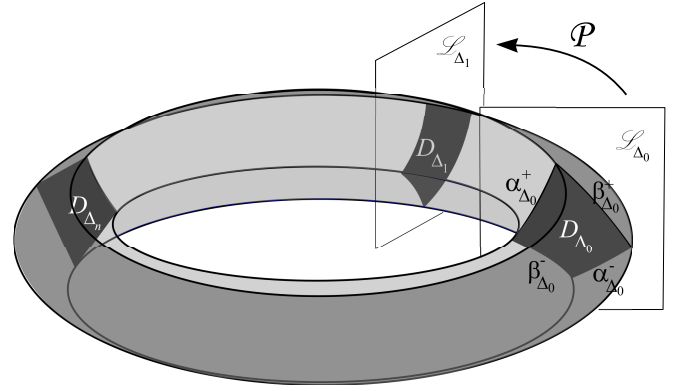


FIG. 2. A  $\gamma$ -donut. For each  $\Delta$ , the intersection of the  $\gamma$ -donut and the plane  $\mathcal{L}_\Delta$  is a  $\gamma$ -island.

Then we call  $\gamma$ -donut the set

$$T = \bigcup_{\Delta \in \mathbb{S}^1} D_\Delta.$$

It follows from the definition that  $T \subseteq \mathcal{U}$ . For any  $\mathbf{p} \in T$  both  $\mathcal{P}(\mathbf{p})$  and  $\mathcal{P}^{-1}(\mathbf{p})$  are defined. The definition of a  $\gamma$ -donut is illustrated in Fig. 2.

**Remark** If  $T$  is a  $\gamma_1$ -donut and  $\gamma_2 > \gamma_1$  then  $T$  is also a  $\gamma_2$ -donut.

**Definition 12** An *alphabet*  $\mathcal{A}_N$  is a finite or countable set of different indices  $i_k$ , also called *letters*. Here,  $N$  denotes the size of the alphabet, which can be a finite integer or (countably) infinite.

**Definition 13** Let  $\mathcal{A}_N$  be an alphabet and  $\gamma > 0$  be fixed. Define  $\gamma$ -donut set as a set  $\mathcal{T} = \bigcup_{i \in \mathcal{A}_N} T^i$  that is a finite or countable union of disjoint  $\gamma$ -donuts.

**Remark** Evidently, if  $N$  is finite and  $T^i$  are  $\gamma_i$ -donuts,  $i \in \mathcal{A}_N$ , then  $\mathcal{T} = \bigcup_{i \in \mathcal{A}_N} T^i$  is a  $\gamma$ -donut set for  $\gamma = \max_{i \in \mathcal{A}_N} \gamma_i$ . Generically, when  $N = \infty$  the set  $\mathcal{T}$  may not be a  $\gamma$ -donut set for any finite  $\gamma$  even if each individual  $T^i$  is a  $\gamma_i$ -donut.

## F. Width of the Strips

Let an  $h_\gamma$ -strip  $H$  lie inside a  $\gamma$ -island  $D_\Delta \subset \mathcal{U}_\Delta$  for some  $\Delta$ .  $H$  is bounded by  $h_\gamma$ -curves  $\alpha_H^+$  and  $\alpha_H^-$ . These curves are graphs of functions  $u' = h_\pm(u)$ . By definition,  $h_\pm(u)$  are  $\gamma$ -Lipschitz functions of the same monotonicity type. Let  $\Theta^\pm$  denote the domains of  $h_\pm(u)$  (see Fig. 3). Generically,  $\Theta^+$  and  $\Theta^-$  do not coincide. Let  $\Theta^+ = [u_0^+; u_1^+]$ ,  $\Theta^- = [u_0^-; u_1^-]$  and

$$u_0 = \min(u_0^-, u_0^+), \quad u_1 = \max(u_1^-, u_1^+).$$

Introduce the new functions  $\tilde{h}_\pm(u)$  as follows

$$\tilde{h}_\pm(u) = \begin{cases} h_\pm(u_0^\pm) & u_0 \leq u \leq u_0^\pm; \\ h_\pm(u) & u \in \Theta^\pm; \\ h_\pm(u_1^\pm) & u_1^\pm \leq u \leq u_1. \end{cases} \quad (13)$$

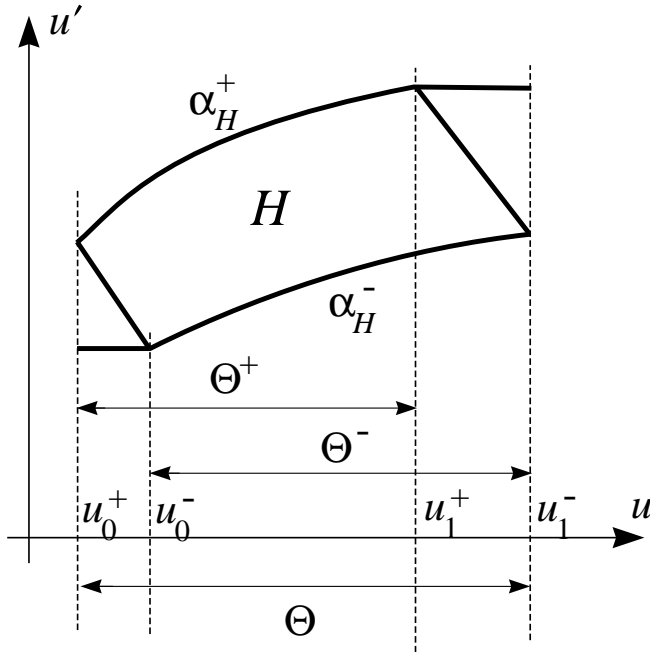


FIG. 3. On the definition of thickness of a strip

Both functions  $\tilde{h}_\pm(u)$  are defined on the same domain  $\Theta = \Theta^+ \cup \Theta^-$ . Since  $h_\pm(u)$  are the  $\gamma$ -Lipschitz functions,  $\tilde{h}_\pm(u)$  are also  $\gamma$ -Lipschitz on  $\Theta$ . Let  $\tilde{\alpha}_H^\pm$  denote the curves which are the graphs of  $\tilde{h}_\pm(u)$ .

**Definition 14** The *thickness* of an  $h_\gamma$ -strip  $H$ , denoted by  $d_h(H)$ , is the  $C$ -norm distance between the curves  $\tilde{\alpha}_H^\pm$ , i.e.

$$d_h(H) = \max_{u \in \Theta} |\tilde{h}_+(u) - \tilde{h}_-(u)|. \quad (14)$$

The thickness of  $v_\gamma$ -strips is defined in the same way. Let a  $v_\gamma$ -strip  $V$  lie inside a  $\gamma$ -island  $D_\Delta$ . Let  $V$  be bounded by the  $v_\gamma$ -curves  $\beta_V^+$  and  $\beta_V^-$ . These curves are the graphs of functions  $u = v_\pm(u')$ . Denote domains of these functions by  $\Theta^\pm$  and continue the functions  $v_\pm(u')$  to the whole interval  $\Theta = \Theta^+ \cup \Theta^-$  in the same way as for  $h_\gamma$ -strips. Introduce the new functions  $\tilde{v}_\pm(u')$  and curves  $\tilde{\beta}_V^\pm$ .

**Definition 15** The *thickness* of a  $v_\gamma$ -strip  $V$ , denoted by  $d_v(V)$ , is the  $C$ -norm distance between the curves  $\tilde{\beta}_V^\pm$ , i.e.

$$d_v(V) = \max_{u' \in \Theta} |\tilde{v}_+(u') - \tilde{v}_-(u')|. \quad (15)$$

### III. SYMBOLIC DYNAMICS

In this section, we formulate sufficient conditions for coding the regular solutions of Eq. (8), i.e.,  $\ddot{u} = G_\delta(x, u)$ , with bi-infinite sequences of letters from a certain alphabet. These conditions are formulated using the auxiliary family of equations given by (11), i.e.,  $\ddot{u} = G_\Delta(x, u)$ , where  $\Delta \in \mathbb{S}^1$  is the parameter. First, we formulate the following two hypotheses.

**Hypothesis 1** The set  $\mathcal{U}$  includes a  $\gamma$ -donut set  $\mathcal{T} = \bigcup_{i \in \mathcal{A}_N} T^i$  for some  $\gamma \geq 0$ , where  $\mathcal{A}_N$  is an alphabet of  $N$  symbols. In addition, there exists a constant  $M$  that for any  $\Delta \in \mathbb{S}^1$  and any  $i \in \mathcal{A}_N$  all islands  $D_\Delta^i = T^i \cap \mathcal{L}_\Delta$  satisfy the following properties:  $d_h(D_\Delta^i) \leq M$  and  $d_v(D_\Delta^i) \leq M$ .

**Hypothesis 2** There exists  $\gamma \geq 0$  such that:

- For each  $i, j \in \mathcal{A}_N$ , for any  $\Delta \in \mathbb{S}^1$  and for any  $h_\gamma$ -strip  $H \subset D_\Delta^i$  the set  $\tilde{H}_j \equiv \mathcal{P}(H) \cap D_{\Delta \oplus 2\theta\pi}^j$  is an  $h_\gamma$ -strip, and there exists  $\rho_h > 1$ , the same for all  $i, j \in \mathcal{A}_N$  and for  $\Delta \in \mathbb{S}^1$ , such that

$$d_h(\tilde{H}_j) \leq d_h(H)/\rho_h. \quad (16)$$

- For each  $i, j \in \mathcal{A}_N$ , for any  $\Delta \in \mathbb{S}^1$  and for any  $v_\gamma$ -strip  $V \subset D_\Delta^j$  the set  $\tilde{V}_i \equiv \mathcal{P}^{-1}(V) \cap D_{\Delta \oplus 2\theta\pi}^i$  is a  $v_\gamma$ -strip, and there exists  $\rho_v > 1$ , the same for all  $i, j \in \mathcal{A}_N$  and for  $\Delta \in \mathbb{S}^1$ , such that

$$d_v(\tilde{V}_i) \leq d_v(V)/\rho_v. \quad (17)$$

**Remark** In particular, Hypothesis 2 implies that both  $\mathcal{P}$ -image and  $\mathcal{P}^{-1}$ -images of any  $\gamma$ -donut from  $\mathcal{T}$  intersect itself and any other  $\gamma$ -donut from  $\mathcal{T}$ . Hypothesis 2 is illustrated in Fig. 4.

**Remark** If Hypotheses 1 and 2 hold for Eq. (8) with some  $\delta \in \mathbb{S}^1$ , then these hypothesis hold for Eq. (8) with *any*  $\delta \in \mathbb{S}^1$ .

Let  $\mathcal{T}$  be a  $\gamma$ -donut set. We use  $\mathcal{O}$  to denote the set of all bi-infinite orbits lying completely in  $\mathcal{T}$ , such that  $\mathbf{p}_0 \in \mathcal{L}_\delta$ . Hence

$$\mathbf{r} \in \mathcal{O} \Leftrightarrow \mathbf{r} = \{\mathbf{p}_n\} \subset \mathcal{T}, \mathcal{P}(\mathbf{p}_n) = \mathbf{p}_{n+1}, \mathbf{p}_0 \in \mathcal{L}_\delta, n \in \mathbb{Z}.$$

The set  $\mathcal{O}$  has the structure of a metric space, where the distance between  $\mathbf{v}, \mathbf{w} \in \mathcal{O}$ ,  $\mathbf{v} = \{\mathbf{p}_n\}$ ,  $\mathbf{w} = \{\mathbf{q}_n\}$  is the Euclidean distance between the points  $\mathbf{p}_0$  and  $\mathbf{q}_0$  in  $\mathcal{L}_\delta$ .

We use  $\mathcal{R}_N$  to denote the set of all bi-infinite sequences  $\{\dots, i_{-1}, i_0, i_1, \dots\}$  where  $i_k, k \in \mathbb{Z}$ , are letters of an alphabet  $\mathcal{A}_N$  of  $N$  symbols (note that  $N$  can be finite or countably infinite, see Definition 12). The set  $\mathcal{R}_N$  has the structure of a topological space, where a system of nested neighborhoods  $W_k(\omega^*)$  of an element  $\omega^* = \{\dots, i_{-1}^*, i_0^*, i_1^*, \dots\} \in \mathcal{R}_N$  is defined as

$$W_k(\omega^*) = \{\omega \mid i_s^* = i_s, |s| < k\}, \quad k = 1, 2, \dots$$

The following theorem establishes that the two hypotheses formulated above provide sufficient conditions for a *homeomorphism* between  $\mathcal{O}$  and  $\mathcal{R}_N$ .

**Theorem 1** Let Hypotheses 1 and 2 be satisfied. Define a map  $\mathcal{C} : \mathcal{O} \rightarrow \mathcal{R}_N$  as follows:  $\mathcal{C}(\mathbf{r}) = \mathbf{s}$ ,  $\mathbf{r} \in \mathcal{O}$ ,  $\mathbf{r} = \{\mathbf{p}_k\}$  and  $\mathbf{s} \in \mathcal{R}_N$ ,  $\mathbf{s} = \{i_k\}$ , such that  $i_k$  is the index of the  $\gamma$ -donut  $T^{i_k} \subset \mathcal{T}$  where the point  $\mathbf{p}_k$  lies. Then  $\mathcal{C}$  is a homeomorphism.

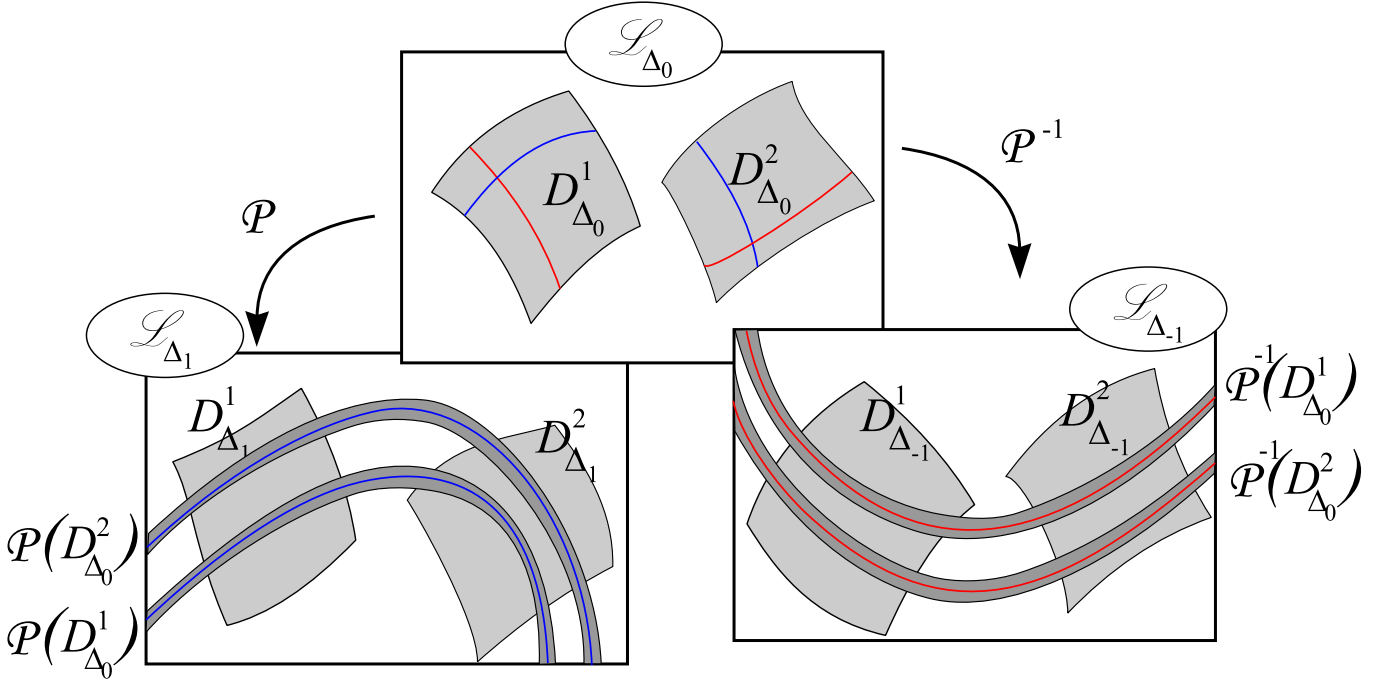


FIG. 4. A sketch illustrating Hypothesis 2. A  $\gamma$ -donut set consists of two donuts,  $T^1$  and  $T^2$ . The plane  $\mathcal{L}_{\Delta_0}$  contains the islands  $D_{\Delta_0}^1$  and  $D_{\Delta_0}^2$  from  $T^1$  and  $T^2$ , respectively. The planes  $\mathcal{L}_{\Delta_{\pm 1}}$  contain the corresponding islands at  $\Delta_1 = \Delta_0 \oplus 2\theta\pi$  and  $\Delta_{-1} = \Delta_0 \ominus 2\theta\pi$ . The images  $\mathcal{P}(D_{\Delta_0}^1)$  and  $\mathcal{P}(D_{\Delta_0}^2)$  intersect the  $\gamma$ -islands  $D_{\Delta_1}^{1,2}$  and each intersection is an  $h$ -strip. Similarly, the pre-images  $\mathcal{P}^{-1}(D_{\Delta_0}^1)$  and  $\mathcal{P}^{-1}(D_{\Delta_0}^2)$  intersect the  $\gamma$ -islands  $D_{\Delta_{-1}}^{1,2}$ , and each intersection is a  $v$ -strip.

**Remark** Theorem 1 generalizes Theorem 1 of Ref.<sup>56</sup> to the quasiperiodic setting. The proof relies on the hyperbolic dynamics of  $\mathcal{P}$ : due to Hypothesis 2 this map contracts strips in one direction while expanding them in another. Such results are standard in symbolic dynamics, with classical references including Refs.<sup>59–61</sup>. Theorem 1 holds regardless of whether the parameter  $\theta$  in the definition of  $G_\delta(x, u)$  is rational or irrational.

Theorem 1 establishes a correspondence between regular on  $\mathbb{R}$  solutions of Eq. (8) and bi-infinite sequences from  $\mathcal{R}_N$ . If  $\mathcal{T} = \mathcal{U}$ , the coding is complete, covering *all* real-valued and regular on  $\mathbb{R}$  solutions  $u(x)$ . If  $\mathcal{T} \neq \mathcal{U}$ ,  $\mathcal{T} \subset \mathcal{U}$ , then the coding may be incomplete, potentially omitting some regular solutions.

**Proof** Evidently, for each bi-infinite orbit  $\mathbf{r} \in \mathcal{O}$  the image  $\mathbf{s} = \mathcal{C}(\mathbf{r})$ ,  $\mathbf{s} \in \mathcal{R}_N$ , is defined uniquely. Let us prove that for each sequence  $\mathbf{s} \in \mathcal{R}_N$  there exists a unique orbit  $\mathbf{r} \in \mathcal{O}$  such that  $\mathbf{s} = \mathcal{C}(\mathbf{r})$ .

Let a sequence  $\mathbf{s} = \{\dots, i_{-1}, i_0, i_1, \dots\}$  be given. Find locations of the points  $\mathbf{p} \in D_\delta^{i_0} \subset T^{i_0}$  such that  $\mathcal{P}^{-1}(\mathbf{p}) \in T^{i-1}$ ,  $\mathcal{P}^{-2}(\mathbf{p}) \in T^{i-2}$ , etc. By definition of  $\mathcal{P}$ ,

$$\mathcal{P}^{-n}(\mathbf{p}) \in D_{\delta \ominus 2\theta n\pi}^{i-n} \subset T^{i-n},$$

where  $D_{\delta \ominus 2\theta n\pi}^{i-n}$  are  $\gamma$ -islands,  $n = 0, 1, \dots$ . By Hypothesis 1 each of these  $\gamma$ -islands satisfies the condition

$$d_h(D_{\delta \ominus 2\theta n\pi}^{i-n}) \leq M, \quad (18)$$

and can be regarded as an  $h_\gamma$ -strip. Initialize a recursive procedure as follows. Since  $i_0$  stands on the zero place in  $\mathbf{s}$  then  $\mathbf{p} \in D_\delta^{i_0}$  where  $D_\delta^{i_0}$  is a  $\gamma$ -island. The points  $\mathbf{p} \in T^{i_0}$  such that  $\mathcal{P}^{-1}(\mathbf{p}) \in T^{i-1}$  are situated in the set  $H_{i-1, i_0} \equiv \mathcal{P}(D_{\delta \ominus 2\theta\pi}^{i-1}) \cap D_\delta^{i_0}$ . Due to Hypothesis 2, the set  $H_{i-1, i_0}$  is an  $h_\gamma$ -strip. Its thickness satisfies the inequality

$$d_h(H_{i-1, i_0}) \leq \rho_h^{-1} d_h(D_{\delta \ominus 2\theta\pi}^{i-1}) \leq \rho_h^{-1} M. \quad (19)$$

The points  $\mathbf{p} \in D_\delta^{i_0}$  such that  $\mathcal{P}^{-1}(\mathbf{p}) \in D_{\delta \ominus 2\theta\pi}^{i-1}$ ,  $\mathcal{P}^{-2}(\mathbf{p}) \in D_{\delta \ominus 4\theta\pi}^{i-2}$  are situated in the set  $H_{i-2, i-1, i_0} \equiv \mathcal{P}(H_{i-2, i-1}) \cap D_\delta^{i_0}$  where  $H_{i-2, i-1} = \mathcal{P}(D_{\delta \ominus 4\theta\pi}^{i-2}) \cap D_{\delta \ominus 2\theta\pi}^{i-1}$ . By Hypothesis 2, the set  $H_{i-2, i-1}$  is an  $h_\gamma$ -strip. Hence, the set  $H_{i-2, i-1, i_0}$  is an  $h_\gamma$ -strip and its thickness satisfies the inequality

$$d_h(H_{i-2, i-1, i_0}) \leq \rho_h^{-1} d_h(H_{i-2, i-1}) \leq \rho_h^{-2} d_h(D_{\delta \ominus 4\theta\pi}^{i-2}) \leq \rho_h^{-2} M.$$

Continuation of this process yields the sequence of nested  $h_\gamma$ -strips,

$$D_\delta^{i_0} \supseteq H_{i-1, i_0} \supseteq H_{i-2, i-1, i_0} \supseteq \dots \quad (20)$$

The thicknesses of these strips tend to zero. The boundaries of the strips are the graphs of  $\gamma$ -Lipschitz functions, so, since the space of the Lipschitz functions is complete (see Remark after Definition 5), the intersection

$$\alpha_\infty \equiv \bigcap_{k=0}^{\infty} H_{i-k, \dots, i-1, i_0} \subset D_\delta^{i_0}$$

is an  $h_\gamma$ -curve.

Consider the sequence of nested  $v_\gamma$ -strips constructed in the same manner,

$$D_\delta^{i_0} \supseteq V_{i_0, i_1} \supseteq V_{i_0, i_1, i_2} \supseteq \dots, \quad (21)$$

where  $V_{i_0, i_1} \equiv \mathcal{P}^{-1}(D_{\delta \oplus 2\theta\pi}^{i_1}) \cap D_\delta^{i_0}$ ,  $V_{i_0, i_1, i_2} \equiv \mathcal{P}^{-1}(V_{i_1, i_2}) \cap D_{\delta \oplus 2\theta\pi}^{i_1}$  where  $V_{i_1, i_2} \equiv \mathcal{P}^{-1}(D_{\delta \oplus 4\theta\pi}^{i_2}) \cap D_{\delta \oplus 2\theta\pi}^{i_1}$ . Their thicknesses are bounded by the sequence  $\{\rho_v^{-n} M\}$ ,  $n = 0, 1, 2, \dots$ , which converges to zero. By the same reasoning as for  $h_\gamma$ -strips, the intersection

$$\beta_\infty \equiv \bigcap_{k=0}^{\infty} V_{i_0, i_1, \dots, i_k} \subset D_\delta^{i_0} \quad (22)$$

is a  $v_\gamma$ -curve.

The orbit  $\mathbf{r} \in \mathcal{O}$  corresponding to the bi-infinite sequence  $\{\dots, i_{-1}, i_0, i_1, \dots\}$  is generated by  $\mathcal{P}$ - and  $\mathcal{P}^{-1}$ -iterations of the intersection  $\alpha_\infty \cap \beta_\infty$  which, according to the definitions of  $h_\gamma$ - and  $v_\gamma$ -curves, consists of one point. Therefore the orbit  $\mathbf{r}$  exists and is unique.

Let us show that the maps  $\mathcal{C}$  and  $\mathcal{C}^{-1}$  are continuous. Since  $\mathcal{P}$  is continuous, if  $\mathbf{r}^{(1)}, \mathbf{r}^{(2)} \in \mathcal{O}$ ,

$$\begin{aligned} \mathbf{r}^{(1)} &= \{\dots, \mathbf{p}_{-1}^{(1)}, \mathbf{p}_0^{(1)}, \mathbf{p}_1^{(1)}, \dots\}, \\ \mathbf{r}^{(2)} &= \{\dots, \mathbf{p}_{-1}^{(2)}, \mathbf{p}_0^{(2)}, \mathbf{p}_1^{(2)}, \dots\}, \end{aligned}$$

are close enough in  $\mathcal{O}$  (i.e. points  $\mathbf{p}_0^{(1)}$  and  $\mathbf{p}_0^{(2)}$  are close in the plane  $\mathcal{L}_\delta$ ), then their  $\mathcal{C}$ -images share the same central block  $|k| < n$  for some  $n$ . Therefore they are also close in  $\mathcal{R}_N$ -topology. Conversely, if  $\mathbf{s}^{(1)} = \mathcal{C}(\mathbf{p}^{(1)})$  and  $\mathbf{s}^{(2)} = \mathcal{C}(\mathbf{p}^{(2)})$  share the same central block  $|k| < n$  for some  $n$  then the points  $\mathbf{p}_0^{(1)}$  and  $\mathbf{p}_0^{(2)}$  are situated in the same domain  $H_{i_{-k}, \dots, i_0} \cap V_{i_0, \dots, i_k}$ , so  $\mathbf{p}_0^{(1)}$  and  $\mathbf{p}_0^{(2)}$  are close in  $\mathcal{O}$ -topology. The theorem is proved.  $\square$

#### IV. STRIP MAPPING THEOREMS

Hypotheses 1 and 2 enable the description of regular solutions for Eq. (8) in terms of coding sequences. However, verifying these hypotheses is challenging, even numerically. This is especially true for Hypothesis 2, as it requires computing the  $\mathcal{P}$ -image of every  $h$ -strip and  $\mathcal{P}^{-1}$ -image of every  $v$ -strip from the given  $\gamma$ -donut set. To simplify the numerical verification of the analogous hypothesis in the periodic setting, in Ref.<sup>56</sup> it was suggested to analyze of the matrix of linearization for the Poincaré map. Two theorems, referred to as *strip mapping theorems*, reduced the verification of Hypothesis 2 to a simple scanning procedure.

The strip mapping theorems can also be generalized to the quasiperiodic setting. Let Hypothesis 1 hold. Let the map  $\mathcal{P}$  and its inverse  $\mathcal{P}^{-1}$  be defined on a  $\gamma$ -donut set  $\mathcal{T} = \bigcup_{i \in \mathcal{A}_N} T^i$  where  $\mathcal{A}_N$  is an alphabet,  $N < \infty$ . For any  $\Delta \in \mathbb{S}^1$  and  $i, j \in \mathcal{A}_N$

define

$$V_{i,j}(\Delta) = \mathcal{P}^{-1}(D_{\Delta \oplus 2\theta\pi}^j) \cap D_\Delta^i,$$

$$H_{i,j}(\Delta) = \mathcal{P}(D_{\Delta \oplus 2\theta\pi}^i) \cap D_\Delta^j.$$

**Remark** The sets  $V_{i,j}$  and  $H_{i,j}$  are related as follows

$$\mathcal{P}(V_{i,j}(\Delta)) = D_{\Delta \oplus 2\theta\pi}^j \cap \mathcal{P}(D_\Delta^i) = H_{i,j}(\Delta \oplus 2\theta\pi) \quad (23)$$

$$\mathcal{P}^{-1}(H_{i,j}(\Delta)) = D_{\Delta \oplus 2\theta\pi}^i \cap \mathcal{P}^{-1}(D_\Delta^j) = V_{i,j}(\Delta \oplus 2\theta\pi). \quad (24)$$

Since Eq. (11) does not include first derivatives, for any fixed  $\Delta \in \mathbb{S}^1$  the map  $\mathcal{P}$  is an area-preserving diffeomorphism from  $V_{i,j}(\Delta) \subset \mathcal{L}_\Delta$  onto  $H_{i,j}(\Delta \oplus 2\theta\pi) \subset \mathcal{L}_{\Delta \oplus 2\theta\pi}$ ,  $i, j \in \mathcal{A}_N$ . Denote by  $\mathcal{D}\mathcal{P}_\mathbf{p}$  the linearization of  $\mathcal{P}$  at  $\mathbf{p} \in V_{i,j}(\Delta)$ ,  $i, j \in \mathcal{A}_N$ . Then for  $\mathbf{p} \in V_{i,j}(\Delta)$  the linear operator  $\mathcal{D}\mathcal{P}_\mathbf{p}$  is represented by  $2 \times 2$  matrix  $(a_{mn})$  and

$$\det[\mathcal{D}\mathcal{P}_\mathbf{p}] = 1. \quad (25)$$

Similarly,  $\mathcal{P}^{-1}$  is also area-preserving, and for any  $\mathbf{q} \in H_{i,j}(\Delta)$ ,  $i, j \in \mathcal{A}_N$ ,

$$\det[\mathcal{D}\mathcal{P}_\mathbf{q}^{-1}] = 1, \quad (26)$$

where  $\mathcal{D}\mathcal{P}_\mathbf{q}^{-1}$  is the linearization of  $\mathcal{P}^{-1}$  at  $\mathbf{q}$ .

**Theorem 2 (On the mapping of h-strips)** Let Hypothesis 1 hold and  $\mathcal{A}_N$  be an alphabet,  $N < \infty$ . Let for any  $\Delta \in \mathbb{S}^1$  and for any pair  $i, j \in \mathcal{A}_N$  the following two conditions be valid:

**(H-1):** one of the following requirements holds:

(A) the borders  $\alpha_i^\pm$  of the island  $D_\Delta^i$  are increasing  $\gamma$ -curves,  $\forall \mathbf{p} \in \overline{V_{i,j}(\Delta)}$  the signs of entries  $\{a_{mn}\}$  in the matrix of the linearization  $\mathcal{D}\mathcal{P}_\mathbf{p} = (a_{mn})$  have exactly one of the following configurations:

$$(a) (+ +), \quad (b) (- -), \quad (c) (+ +), \quad (d) (- -)$$

and at the same time the borders  $\alpha_j^\pm$  of  $D_{\Delta \oplus 2\theta\pi}^j$  are increasing  $\gamma$ -curves for cases (a), (b), and decreasing  $\gamma$ -curves for (c), (d);

(B) the borders  $\alpha_i^\pm$  of the island  $D_\Delta^i$  are decreasing  $\gamma$ -curves,  $\forall \mathbf{p} \in \overline{V_{i,j}(\Delta)}$  signs of  $\{a_{mn}\}$  in the matrix of the linearization  $\mathcal{D}\mathcal{P}_\mathbf{p}$  have exactly one of the following configurations:

$$(a) (+ -), \quad (b) (- +), \quad (c) (+ -), \quad (d) (- +)$$

and at the same time borders  $\alpha_j^\pm$  of  $D_{\Delta \oplus 2\theta\pi}^j$  are decreasing  $\gamma$ -curves for cases (a), (b), and increasing for (c), (d).

**(H-2):** there exists  $\rho_h > 1$  such that for any  $\mathbf{p} \in \overline{V_{i,j}(\Delta)}$ ,  $|a_{11}| \geq \rho_h$ .

Then

**(H-i)** for any  $h_\gamma$ -strip  $H \subset D_\Delta^i$  there exists  $\gamma_j$  (independent on  $\Delta$ ) such that  $\mathcal{P}(H) \cap D_{\Delta \oplus 2\theta\pi}^j = \tilde{H}^j$  is also an  $h_{\gamma_j}$ -strip;  
**(H-ii)**  $d_h(\tilde{H}^j) \leq d_h(H)/\rho_h$ .

**Remark** The signs “+” and “-” mean that the *strict* inequalities  $a_{mn} > 0$  and  $a_{mn} < 0$  must hold, respectively.

**Proof** The proof follows step-by-step the proof of Theorem 2 for periodic case in Ref.<sup>56</sup> (section 5). The only difference is that in the periodic case, the Poincaré map sends  $\mathbb{R}^2$  to itself, whereas in our case, its counterpart  $\mathcal{P}$  maps a  $\Delta$ -slice to a  $(\Delta \oplus 2\theta\pi)$ -slice for each  $\Delta \in \mathbb{S}^1$ . Let us sketch the proof. At the first step, one shows that under the conditions of the theorem  $\mathcal{P}$  preserves Lipschitz and monotonicity properties when mapping the curves from  $V_{i,j}(\Delta) \subset D_\Delta^i$  to  $D_{\Delta \oplus 2\theta\pi}^j$ . At the second step one uses this fact to prove that for any  $h_\gamma$ -strip  $H \subset D^i(\Delta)$  its  $\mathcal{P}$  image  $\tilde{H}^j \subset D_{\Delta \oplus 2\theta\pi}^j$  is also a  $h_{\gamma_j}$ -strip for some  $\gamma_j$ . Finally, one shows that the condition (H-2) implies that  $\mathcal{P}$  contracts the  $h$ -strips.  $\square$

**Theorem 3 (On the mapping of v-strips)** Let Hypothesis 1 hold and  $\mathcal{A}_N$  be an alphabet,  $N < \infty$ . Let for any  $\Delta \in \mathbb{S}^1$  and for any pair  $i, j \in \mathcal{A}_N$  the following two conditions be valid:

**(V-1):** one of the following conditions hold:

(A) the borders  $\beta_j^\pm$  of the island  $D_\Delta^j$  are increasing  $\gamma$ -curves,  $\forall \mathbf{q} \in \overline{H_{i,j}(\Delta)}$  the signs of entries  $\{b_{mn}\}$  in the matrix of the linear operator  $\mathcal{D}\mathcal{P}_{\mathbf{q}}^{-1} = (b_{mn})$  have exactly one of the following configurations:

$$(a) (+ +), \quad (b) (- -), \quad (c) (+ -), \quad (d) (- +)$$

and at the same time the borders  $\beta_i^\pm$  of  $D_{\Delta \oplus 2\theta\pi}^i$  are increasing  $\gamma$ -curves for cases (a), (b), and decreasing  $\gamma$ -curves for (c), (d);

(B) the borders  $\beta_j^\pm$  of an island  $D_\Delta^j$  are decreasing  $\gamma$ -curves,  $\forall \mathbf{q} \in \overline{H_{i,j}(\Delta)}$  signs of  $\{b_{mn}\}$  in the matrix of the linear operator  $\mathcal{D}\mathcal{P}_{\mathbf{q}}^{-1} = (b_{mn})$  have exactly one of the following configurations:

$$(a) (+ -), \quad (b) (- +), \quad (c) (+ -), \quad (d) (- +)$$

and at the same time borders  $\beta_i^\pm$  of  $D_{\Delta \oplus 2\theta\pi}^i$  are decreasing  $\gamma$ -curves for cases (a), (b), and increasing for (c), (d).

**(V-2):** there exists  $\rho_v > 1$  such that for any  $\mathbf{q} \in \overline{H_{i,j}(\Delta)}$ ,  $|b_{22}| \geq \rho_v$ .

Then

**(V-i)** for any  $v_\gamma$ -strip  $V \subset D_\Delta^i$  there exists  $\gamma_j$  (independent on  $\Delta$ ) such that  $\mathcal{P}^{-1}(V) \cap D_{\Delta \oplus 2\theta\pi}^j = \tilde{V}^j$  is also an  $v_{\gamma_j}$ -strip;  
**(V-ii)**  $d_v(\tilde{V}^j) \leq d_v(V)/\rho_v$ .

The proof of Theorem 3 repeats the steps of the proof of Theorem 2 to  $v_\gamma$ -strips.

Theorems 2 and 3 are equivalent in the following sense.

**Theorem 4** Let Hypothesis 1 hold and  $\mathcal{A}_N$  be an alphabet,  $N < \infty$ . Then the conditions (H-1) and (H-2) of Theorem 2 imply the conclusions (V-i) and (V-ii) of Theorem 3. Conversely, the conditions (V-1) and (V-2) of Theorem 3 imply the conclusions (H-i) and (H-ii) of Theorem 2.

**Proof** Due to relations (23) and (24), if  $\mathbf{p} \in \overline{V_{i,j}(\Delta)}$ ,  $\Delta \in \mathbb{S}^1$ , then  $\mathbf{q} = \mathcal{P}(\mathbf{p}) \in \overline{H_{i,j}(\Delta)}$  where  $\Delta_1 = \Delta \oplus 2\theta\pi$ . Let  $\mathcal{D}\mathcal{P}_{\mathbf{p}} = \begin{pmatrix} a_{11} & a_{12} \\ a_{21} & a_{22} \end{pmatrix}$  satisfy the conditions (A) or (B) of Theorem 2. Since  $\det[\mathcal{D}\mathcal{P}_{\mathbf{p}}] = 1$ , for  $\mathbf{q} \in \overline{H_{i,j}(\Delta)}$

$$\mathcal{D}\mathcal{P}_{\mathbf{q}}^{-1} = [\mathcal{D}\mathcal{P}_{\mathbf{p}}]^{-1} = \begin{pmatrix} a_{22} & -a_{12} \\ -a_{21} & a_{11} \end{pmatrix} = \begin{pmatrix} b_{11} & b_{12} \\ b_{21} & b_{22} \end{pmatrix}.$$

So, the signs of  $(b_{mn})$  agree with conditions for  $\mathbf{q} \in \overline{H_{i,j}(\Delta)}$  of Theorem 3 for any  $\Delta \in \mathbb{S}^1$ . Then the corresponding set of signs for  $\mathcal{D}\mathcal{P}_{\mathbf{q}}^{-1}$ , either (A) or (B), in Theorem 3 holds and  $|b_{22}| = |a_{11}| \geq \rho_h > 1$ . The converse statement, that the conditions of Theorem 3 imply the conclusions of Theorem 2, is proved similarly.  $\square$

By Theorem 4, Hypothesis 2 is satisfied if the conditions of either Theorem 2 or Theorem 3 hold. From a practical standpoint, verifying the conditions of either of these theorems is significantly simpler than directly checking Hypothesis 2. Rather than studying the images of all  $h$ - and  $v$ -strips the analysis reduces to examining the linearization matrices  $\mathcal{D}\mathcal{P}_{\mathbf{p}}$  or  $\mathcal{D}\mathcal{P}_{\mathbf{q}}^{-1}$  at points  $\mathbf{p}, \mathbf{q}$  within the donut set.

## V. NUMERICAL VERIFICATION OF THE HYPOTHESES

The conditions of Hypotheses 1 and 2 can be checked using numerical computations. To this end, we select the scanning domain  $\Omega \subset \mathcal{L}$ .

$$\Omega = \{(\Delta, u, u') \mid 0 \leq \Delta < 2\pi, -U \leq u \leq U, -U' \leq u' \leq U'\}.$$

The domain  $\Omega$  is chosen to be large enough to fully encompass the set  $\mathcal{U}$ , whenever possible. We introduce in  $\Omega$  a uniform 3D-grid  $(\Delta_k, u_l, u'_m)$ ,  $k = 1, \dots, N_\Delta$ ,  $l = -N_u, \dots, N_u$ ,  $m = -N_{u'}, \dots, N_{u'}$ . The computation consists of two steps.

In the first step, we verify the conditions of Hypothesis 1. We compute a grid approximation of the set  $\mathcal{U} \cap \Omega$  to obtain numerical evidence that  $\mathcal{U}$  contains a  $\gamma$ -donut set. For this purpose, we select points in  $\Omega$  for which both  $\mathcal{P}$  and  $\mathcal{P}^{-1}$  exist. For each fixed  $k$ , we take  $\Delta = \Delta_k$  and use  $(u_l, u'_m)$ ,  $l = -N_u, \dots, N_u$ ,  $m = -N_{u'}, \dots, N_{u'}$  as initial data for the Cauchy problem

$$\ddot{u} = G_{\Delta_k}(x, u), \quad u(0) = u_l, \quad \dot{u}(0) = u'_m. \quad (27)$$

The problem (27) is solved numerically. If the solution to (27) exists on the interval  $[0, 2\pi]$ , then the image  $\mathcal{P}(\mathbf{p})$  is defined

for the grid node  $\mathbf{p} = (\Delta_k, u_l, u'_m)$ . Thus, this node belongs to the grid approximation of the set  $\mathcal{U}_{\Delta_k}^+ \cap \Omega$ . Similarly, we obtain the grid approximation of the set  $\mathcal{U}_{\Delta_k}^- \cap \Omega$  by selecting the nodes for which the solution to (27) can be extended to the interval  $[-2\pi; 0]$ . Then we compute the intersection of these sets, that is  $\mathcal{U}_{\Delta_k} \cap \Omega$ . Hypothesis 1 holds if for any  $\Delta_k$ ,  $k = 1, \dots, N_\Delta$ , the set  $\mathcal{U}_{\Delta_k} \cap \Omega$  includes a finite number of  $\gamma$ -islands (for some  $\gamma$  independent of  $k$ ), and the monotonic properties of the islands' boundaries are the same for all  $\Delta_k$ .

If the first step is successful, we proceed to the second step: the numerical verification of Hypothesis 2. The base for this is provided by Theorems 2 and 3 which apply to the case when the  $\gamma$ -donut set consists of a finite number of  $\gamma$ -donuts. Due to Theorem 4, it is enough to check the conditions of only one of these theorems. We have used Theorem 2. On an adapted grid from the prior scan, for any fixed  $\Delta_k$  we solve the Cauchy problem (27) and select the grid nodes for which the solution can be extended to the interval  $[-2\pi; 4\pi]$ . For any such node  $\mathbf{p} = (\Delta_k, u_l, u'_m)$  both  $\mathcal{P}^2 \mathbf{p}$  and  $\mathcal{P}^{-1} \mathbf{p}$  exist. Thus this node belongs to the numerical approximation of the set  $\bigcup_{i,j} V_{i,j}(\Delta_k) \cap \Omega$ . For any node  $\mathbf{p}$  of this set we compute the matrix of linearization  $\mathcal{D}\mathcal{P}_{\mathbf{p}} = (a_{11} \ a_{12} \ a_{21} \ a_{22})$ . We store the signs of its entries together with the value of  $a_{11}$ . Then one has to ensure that the conditions (H-1) and (H-2) hold for any pair  $i, j \in \mathcal{A}_N$ .

The procedure is repeated for any  $\Delta_k$ ,  $k = 1, \dots, N_\Delta$ . If the points (H-1) and (H-2) hold for any  $\Delta_k$  we conclude that the conditions of Hypotheses 2 are valid.

Algorithm 1 summarizes the procedure for verification of Hypotheses 1 and 2. Illustrations of this procedure are provided in Sec. VI.

---

**Algorithm 1** Numerical Check of Hypotheses 1 and 2

---

**Input:** The scanning area

$$\Omega = \{(\Delta, u, u') \mid 0 \leq \Delta < 2\pi, -U \leq u \leq U, -U' \leq u' \leq U'\}.$$

covered by a uniform 3D grid

$$(\Delta_k, u_l, u'_m), \ k = 1, \dots, N_\Delta, \ l = -N_u, \dots, N_u, \ m = -N_{u'}, \dots, N_{u'}.$$

**Step 1: Verify Hypothesis 1.**

**(i) Grid approximation of  $\mathcal{U} \cap \Omega$ .** For each  $(k, l, m)$ :

Solve Eq. (27) with initial data  $u(0) = u_l$ ,  $\dot{u}(0) = u'_m$ . Store the sets  $\Omega_k$ ,  $k = 1, \dots, N_\Delta$ , that consist of pairs  $(u_l, u'_m)$  corresponding to solutions  $u(x)$  that are regular on  $x \in [-2\pi; 2\pi]$ .

**(ii) Searching for islands in  $\Delta$ -slices.** For each  $\Delta_k$ ,  $k = 1, \dots, N_\Delta$ , separate connected components in each  $\Omega_k$ , selecting those that correspond to  $\gamma$ -islands.

**(iii) Searching for a donut set.** Select islands that form donuts as  $k$  runs from 1 to  $N_\Delta$ . Introduce  $N$  — the number of donuts in the donut set, and enumerate the donuts using indices  $i$  from an  $N$ -symbol alphabet  $\mathcal{A}_N$ .

**Step 2: Verify Hypothesis 2.**

For each  $k = 1, \dots, N_\Delta$  repeat the following steps:

**(i)** For each  $i$  from  $\mathcal{A}_N$ , and for each  $\mathbf{p} = (\Delta_k, u_l, u'_m)$  from  $D_{\Delta_k}^i$ :  
Solve Eq. (27) for initial data  $u(0) = u_l$ ,  $\dot{u}(0) = u'_m$ . If the solution  $u(x)$  is regular on  $[-2\pi, 4\pi]$ , then store the following data:

- the pair  $(i, j)$ , where  $j \in \mathcal{A}_N$  is the index of the donut containing the point  $(\Delta_k \oplus 2\pi\theta, u(2\pi), u'(2\pi))$ ;
- the  $2 \times 2$  linerization matrix  $\mathcal{D}\mathcal{P}_{\mathbf{p}} = (a_{m,n})_{m,n=1,2}$ ;

**(ii)** Check that the pairs stored at the previous step contain every element of  $\mathcal{A}_N \times \mathcal{A}_N$ ;

**(iii)** For all stored linearization matrices, check that the signs of their entries  $a_{mn}$  meet the conditions of Theorem 2;

**(iv)** Compute  $\rho_* = \min |a_{11}|$  over all stored linearization matrices and check that  $\rho_* > 1$ .

If conditions corresponding to steps (ii), (iii), (iv) hold for every  $k$ , then Hypothesis 2 is satisfied

---

## VI. EXAMPLES

We exemplify this procedure using Eq. (3) with the quasiperiodic potential, see the setting (5). In this case the equation reads

$$\ddot{u} + (\mu + A_1 \cos 2x + A_2 \cos(2\theta x + \delta)) u - u^3 = 0. \quad (28)$$

Here the phase shift  $\delta$  is fixed,  $\delta \in [0, 2\pi)$ ,  $\theta > 1$  is an irrational number. In the examples below, we use the golden ratio  $\theta = (\sqrt{5} + 1)/2$ . In the context of BEC,  $\mu$  represents the chemical potential and  $A_{1,2}$  are the amplitudes of the laser beams that form the quasiperiodic lattice. The independent variable  $x$  has been scaled to make the linear part of Eq. (28) consistent with the Mathieu equation. Then the map  $\mathcal{P}$  is defined over the period of one of cosines, i.e., for  $x \in [0; \pi]$ , instead of  $x \in [0; 2\pi]$ . So,  $\mathcal{P}$  is defined as follows:  $\mathcal{P}(\mathbf{p}_0) = \mathbf{p}_1$  where  $\mathbf{p}_0 = (\Delta_0, u_0, u'_0)$ ,  $\mathbf{p}_1 = (\Delta_1, u_1, u'_1)$  and

- $\Delta_1 = \Delta_0 \oplus 2\theta\pi$ ;
- $u_1 = u(\pi)$ ,  $u'_1 = \dot{u}(\pi)$  where  $u(x)$  is the solution of the Cauchy problem for Eq. (11) with  $\Delta = \Delta_0$  and initial data  $u(0) = u_0$ ,  $\dot{u}(0) = u'_0$ .

**Example 1** Consider Eq. (28) with  $\mu = 1$ ,  $A_1 = 3$ ,  $A_2 = 2$  and  $\delta = 0$ . The set  $\mathcal{U}$  has been computed by scanning the domain  $\Omega \subset \mathcal{L}$  on a grid of  $16 \times 2000 \times 2000$  nodes. Figure 5 shows the sets  $\mathcal{U}_{\pi k/4}^+$  (dark gray),  $\mathcal{U}_{\pi k/4}^-$  (light gray) and  $\mathcal{U}_{\pi k/4}$  (black),  $k = 0, \dots, 7$ . The sets  $\mathcal{U}_{\pi k/4}$  are the cross-sections of the set  $\mathcal{U} \subset \mathcal{L}$  by the  $\Delta$ -slices, where  $\Delta = \pi k/4$ . Each  $\Delta$ -slice contains three  $\gamma$ -islands ( $\gamma$  is finite). We introduce an alphabet  $\mathcal{A}_3 = \{-1, 0, 1\}$  and label the islands as  $D_{\Delta}^{-1}$ ,  $D_{\Delta}^0$  and  $D_{\Delta}^1$ . Without loss of generality, we use  $D_{\Delta}^0$  to denote the  $\gamma$ -island that contains the origin  $(u, u') = (0, 0)$ . Since for  $\delta = 0$  the quasiperiodic potential is an even function of  $x$ , the other two islands,  $D_{\Delta}^{-1}$  and  $D_{\Delta}^1$ , are mirrored copies of one another with respect to the origin  $(u, u') = (0, 0)$ . Each of the islands undergoes a continuous deformation when  $\Delta$  varies, conserving the monotonic properties of its  $\alpha$ - and  $\beta$ -boundaries. So, in  $\mathcal{L}$  each of these three islands generates a  $\gamma$ -donut. Therefore, we conclude that the set  $\mathcal{U}$  contains a  $\gamma$ -donut set  $\mathcal{T}$ . This yields numerical evidence supporting Hypothesis 1. Enlarging the scanning area  $\Omega$  does not reveal other intersections of  $\mathcal{U}_{\Delta}^+$  and  $\mathcal{U}_{\Delta}^-$ . This indicates that  $\mathcal{U} = \mathcal{T}$ .

The next step involves the analysis of  $h$ - and  $v$ -strips. To find  $V_{i,j}(\Delta)$ ,  $i, j \in \mathcal{A}_3$ , we scan the islands in a fixed  $\Delta$ -slice identifying points that have a  $\mathcal{P}^2$ -image. By definition,  $V_{i,j}(\Delta)$  is a  $v$ -strip which is situated in the island  $D_{\Delta}^j$  and mapped by  $\mathcal{P}$  to the island  $D_{\Delta \oplus 2\pi\theta}^j$ . We also compute  $h$ -strips  $H_{i,j}(\Delta)$  selecting the points in the islands in  $\Delta$ -slice that have a  $\mathcal{P}^{-2}$ -image. By definition,  $H_{i,j}(\Delta)$  is an  $h$ -strip which is situated in the island  $D_{\Delta}^j$  and mapped by  $\mathcal{P}^{-1}$  into  $D_{\Delta \oplus 2\pi\theta}^i$ . Figure 6 shows the strips for  $\Delta = 0$ , i.e.,  $V_{i,j}(0)$  and  $H_{i,j}(0)$ .

To check the conditions of Theorem 2, for any grid point  $\mathbf{p} \in V_{i,j}(\Delta)$  and for any  $\Delta = \Delta_k \in [0; 2\pi]$  we compute the matrices  $\mathcal{D}\mathcal{P}_{\mathbf{p}}$ . Since this computation involves only the points within the  $\gamma$ -islands, we perform this procedure on a finer numerical grid than that used for verifying Hypothesis 1. The result is shown in Fig. 7, where we use different colors to represent different combinations of signs for the entries of the linearization matrices. For each considered  $v$ -strip  $V_{i,j}(\Delta)$ , the linearization satisfies the requirements of Theorem 2. To complete the verification of the conditions of this theorem, for each island  $D_{\Delta}^{-1}$ ,  $D_{\Delta}^0$ , and  $D_{\Delta}^1$ , we additionally compute  $\rho_h$  as

$$\min_{\mathbf{p} \in V_{-1,j}(\Delta)} |a_{11}|, \quad \min_{\mathbf{p} \in V_{1,j}(\Delta)} |a_{11}|, \quad \min_{\mathbf{p} \in V_{0,j}(\Delta)} |a_{11}|.$$

Here  $j = -1, 0, 1$  and  $\Delta \in [0; 2\pi]$ . The result is plotted in Fig. 8. For each island, we find  $\rho_h > 1$ , providing numerical support for the validity of Theorem 2 and, consequently, of Hypothesis 2.

Since both Hypotheses 1 and 2 have been numerically verified, we conclude that there exists a one-to-one correspondence between all bi-infinite sequences over the three-symbol

alphabet  $\mathcal{A}_3 = \{-1, 0, 1\}$  and the regular and real-valued solutions of Eq. (28) for the given parameters. This correspondence implies that for any sequence  $(\dots, i_{-1}, i_0, i_1, \dots)$ ,  $i_k \in \mathcal{A}_3$ , there exists a unique solution of Eq. (28) such that  $(\delta \oplus 2k\pi\theta, u(k\pi), \dot{u}(k\pi)) \in T^{i_k}$ ,  $k \in \mathbb{Z}$ . Moreover, since our computations confirm that  $\mathcal{U} = \mathcal{T}$  we conclude that all regular solutions of Eq. (28) are in one-to-one correspondence with these bi-infinite codes. This means that for any regular solution of Eq. (28) there exists the coding sequence  $(\dots, i_{-1}, i_0, i_1, \dots)$ ,  $i_k \in \mathcal{A}_3$ .

Figure 9(a) shows four solutions that correspond to the codes  $(\dots, \underline{0}, 1, 0, \dots)$ ,  $(\dots, \underline{0}, 0, 1, 0, \dots)$ ,  $(\dots, \underline{0}, 0, 0, 1, 0, \dots)$ , and  $(\dots, \underline{0}, 0, 0, 0, 1, 0, \dots)$ , where we use the underline to denote  $i_0$ . Each solution is localized at a local minima of the quasiperiodic potential. The lack of translational invariance implies that all displayed solutions are distinct, despite their codes differing only in the location of the symbol “1” relative to  $i_0 = \underline{0}$ . The coding approach can also be applied to more complex solutions: in Fig. 9(b), we show the solutions with the codes  $(\dots, \underline{0}, 1, 1, 0, 0, \dots)$  and  $(\dots, \underline{0}, 0, 0, 1, 1, 0, \dots)$ .

Let us briefly discuss the range of the parameters where the established coding can be applied. First, we recall that the validity of Hypotheses 1 and 2 for  $\delta = 0$  imply that the same hypotheses remain valid for any  $\delta \in [0; 2\pi]$ , see the remark in Sec. III. In addition, we fulfilled the same numerical check for  $\mu = 1$ ,  $A_1 = 3$ , and various values of  $A_2$ . Our computations show that Hypotheses 1 and 2 hold if  $0 \leq |A_2| \leq 2.5$ . Note that at  $A_2 = 0$  the potential becomes periodic, and the coding approach reduces to that introduced in Ref.<sup>51</sup>.

It is instructive to compare our results with those obtained using rational approximations of the golden ratio  $\theta$ , a common technique for quasiperiodic problems<sup>8,14,15,18,20,43–45</sup>. We applied our method to Eq. (28) with  $\theta$  replaced by the rational approximations  $21/13$  and  $55/34$ , where the numerator and denominator of each fraction are successive Fibonacci numbers. In both cases, the potential  $V(x)$  becomes periodic, with periods  $13\pi$  and  $34\pi$ , respectively. For both approximations, we observed no appreciable difference from the results for the original quasiperiodic potential. Specifically, with identical parameters  $(\mu, A_1, A_2)$ , three islands appear in each  $\Delta$ -slice ( $\Delta \in [0, 2\pi]$ ), corresponding to three donuts in the full space  $\mathcal{L}$ . Analysis of the strips  $V_{i,j}$  shows that Hypothesis 2 also holds. Therefore, there exists the one-to-one correspondence between all bi-infinite sequences over the three-symbol alphabet  $\mathcal{A}_3 = \{-1, 0, 1\}$  and the regular, real-valued solutions of Eq. (28) where  $\theta$  is replaced by its rational approximation. This implies, in particular, that  $\mu = 1$  must lie within the spectral gaps of both approximate periodic potentials. If this were not the case, the behavior of  $\mathcal{P}$  in vicinity of the origin  $(0, 0)$  would not be hyperbolic, and the matrix  $\mathcal{D}\mathcal{P}_{(0,0)}$  would fail to satisfy conditions (H-1)(H-2). However, one cannot generally exclude the situation where a given  $\mu$  falls within a spectral gap for one approximate potential but lies in an allowed band for the other.

To demonstrate that the one-to-one correspondence established in Example 1 is not trivial and does not hold by default, below we provide two examples where one of the hypotheses fails, and consequently, the coding procedure is not directly

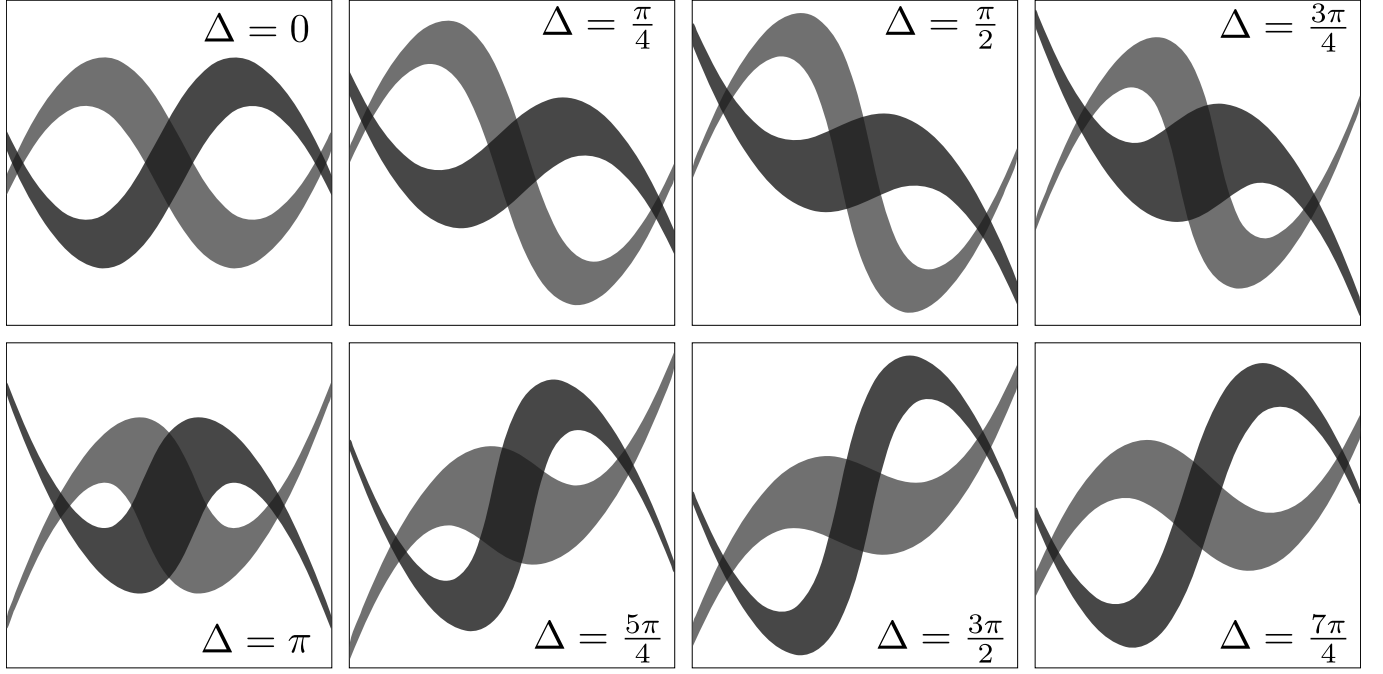


FIG. 5. Numerical verification of Hypothesis 1 for Example 1. Each panel shows the sets  $\mathcal{U}_{\pi k/4}^+$  (dark gray),  $\mathcal{U}_{\pi k/4}^-$  (light gray) and  $\mathcal{U}_{\pi k/4}$  (black). For each  $\Delta$ , there are exactly three  $\gamma$ -islands and each  $\gamma$ -island continuously changes with  $\Delta$ . Each panel shows the region  $(u, u') \in [-2; 2] \times [-2; 2]$ .

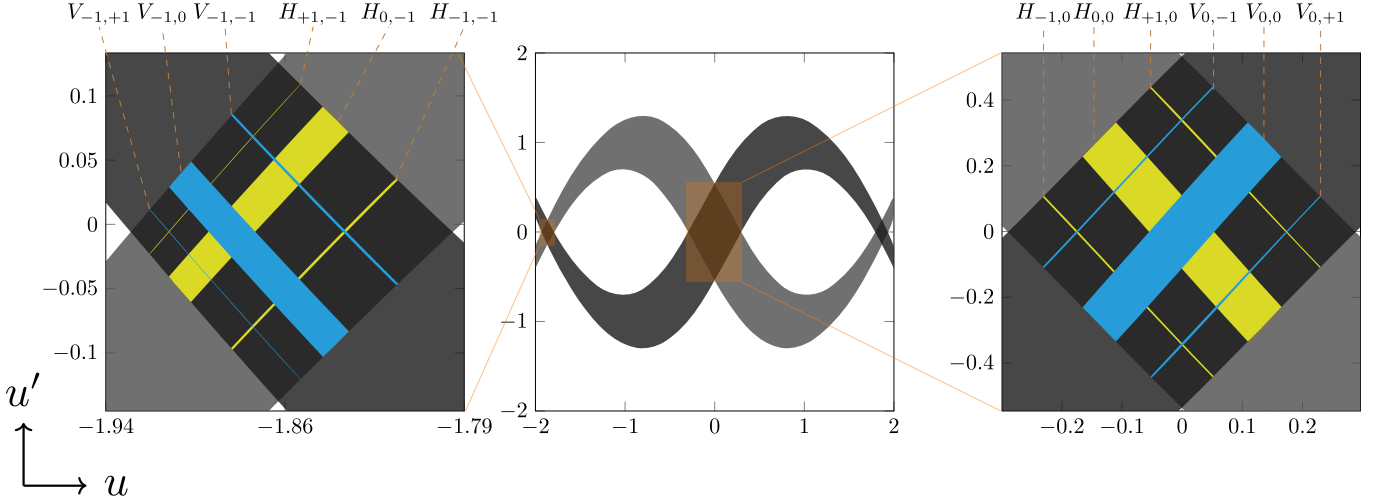


FIG. 6. Example 1: the positions of the islands in  $\Delta$ -slice with  $\Delta = 0$  (central panel) and the  $v$ -strips  $V_{i,j}(0)$  (blue) and  $h$ -strips  $H_{i,j}(0)$  (yellow). Left and right panels show the island  $D_0^{-1}$  and  $D_0^0$ , respectively. The island  $D_0^1$  is not shown, as it is symmetric to  $D_0^{-1}$  with respect to the origin.

applicable.

**Example 2** If in Eq. (28) we take  $\mu = 0.4$ , while keeping  $A_1 = 3$ ,  $A_2 = 2$  and  $\delta = 0$  as in Example 1, the situation changes qualitatively. Figure 10 shows the sets  $\mathcal{U}_\Delta^+$  (dark gray),  $\mathcal{U}_\Delta^-$  (light gray) for  $\Delta = 0$  and  $\pi$ . For  $\Delta = \pi$ , the intersection  $\mathcal{U}_\Delta$  (black) can not be represented as an union of disjoint islands. Consequently, the set  $\mathcal{U}$  is not a donut set, and the conditions of Hypothesis 1 are not satisfied. Thus, the

coding procedure does not apply in this case.

**Example 3** For the parameters of Example 1 but with  $\mu = 1.8$  instead of  $\mu = 1$ , the island structure persists in every  $\Delta$ -slice which indicates that Hypothesis 1 holds. However, checking the entries in the matrices  $\mathcal{DP}_p$  reveals that their signs do not satisfy the conditions of Theorem 2 (see Fig. 11). Therefore, we cannot claim that Hypothesis 2 also holds, and our coding procedure is again inapplicable.

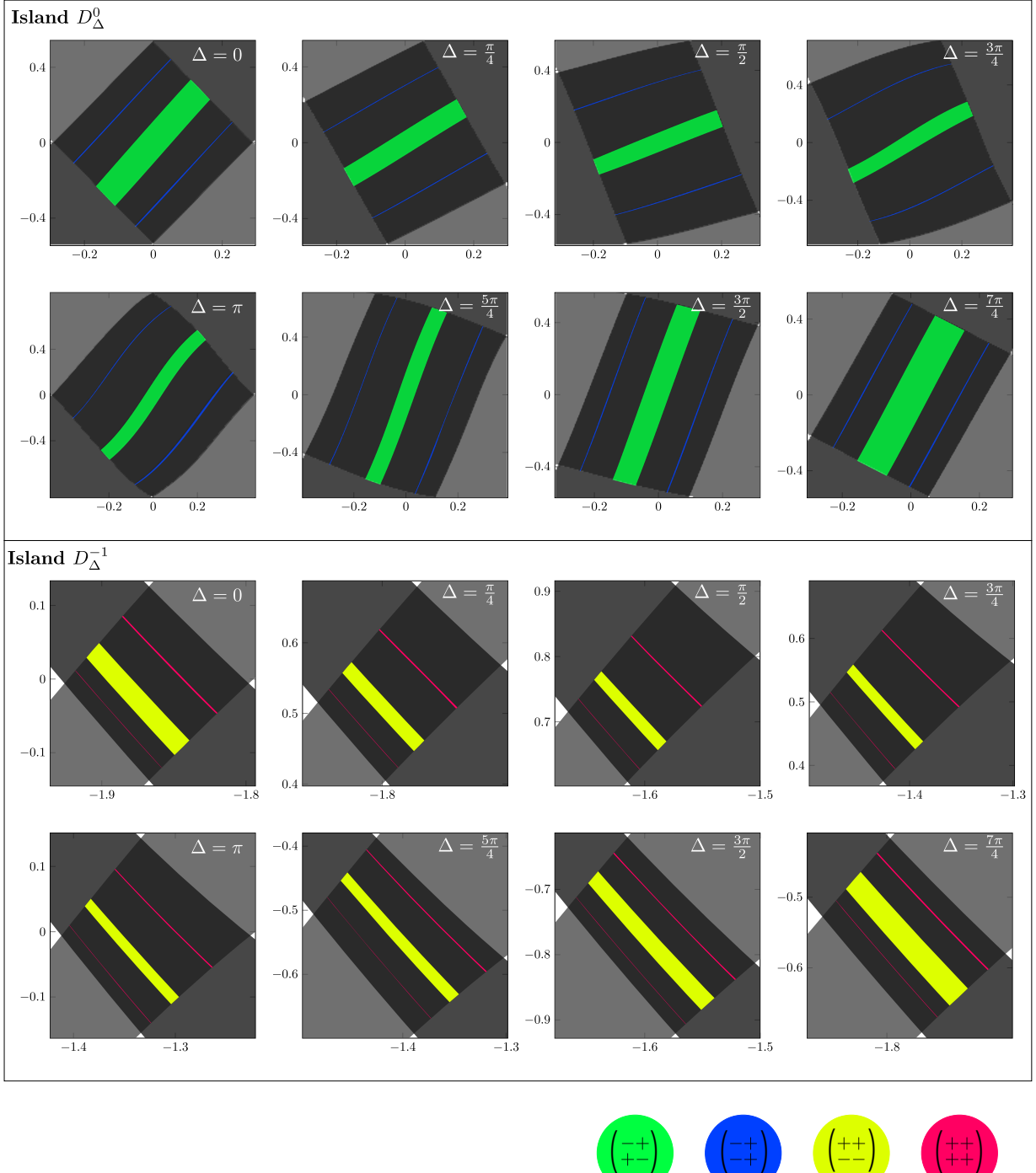


FIG. 7. Numerical verification of Hypothesis 2 for Example 1. Each panel shows  $v$ -strips  $V_{i,j}(\Delta)$ ,  $i, j \in \{-1, 0, 1\}$  in the island  $D_\Delta^0$  (upper panel) and  $D_\Delta^{-1}$  (lower panel), for  $\Delta = k\pi/4$ ,  $k = 0, 1, \dots, 7$ . The configurations of signs in the linearization matrices  $\mathcal{D}\mathcal{P}_p$  are represented by different colors, see the color legend under the main panels.

## VII. ALTERNATIVE INTERPRETATION OF THE CODING APPROACH

Here we provide a heuristic interpretation of our mathematical results on coding of nonlinear states in a quasiperiodic potential. This interpretation builds upon known results re-

garding the solutions of the equation

$$u_{xx} + (\mu - V(x))u - u^3 = 0. \quad (29)$$

Let  $\mu$  be fixed. We split the explanation into the following steps.

1. Let  $V(x)$  be a single-well potential of finite depth (see

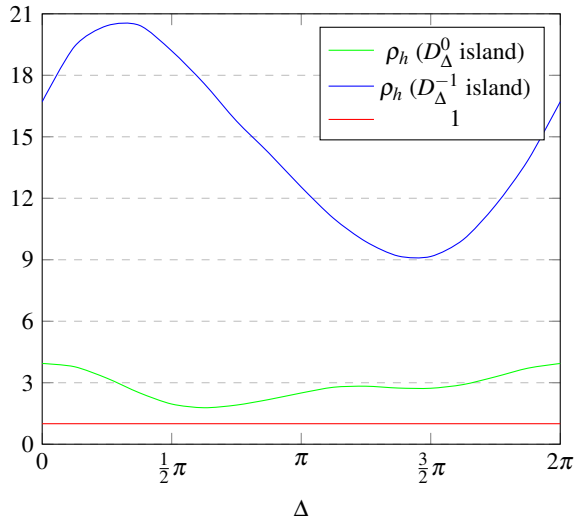


FIG. 8. Values of  $\rho_h$  for  $D_\Delta^{-1}$  and  $D_\Delta^0$  for Example 1. The values of  $\rho_h$  for  $D_\Delta^1$  are the same as for  $D_\Delta^{-1}$  since these islands are symmetric to each other with respect to the origin.

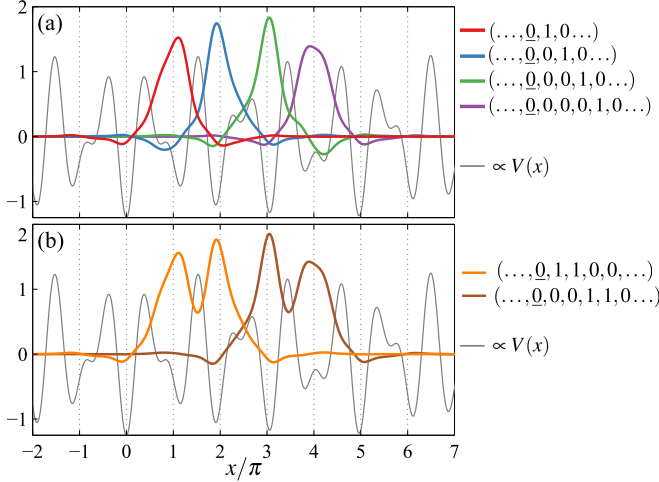


FIG. 9. Example 1: solutions  $u(x)$  with codes that contain exactly one nonzero symbol (a) and exactly two nonzero symbols (b). Thin gray lines plot the quasiperiodic lattice (up to a scaling factor).

Fig. 12A,B). Consider localized solutions of (29) such that

$$u(x) \rightarrow 0, \quad x \rightarrow \pm\infty.$$

Evidently,  $u(x) \equiv 0$  is a solution of Eq. (29). Also, if  $u(x)$  is a solution of Eq. (29) then  $-u(x)$  is also a solution of this equation. The total number of localized solutions is finite, odd and determined by the width and the depth of the potential  $V(x)$ . We note that arguments for a finite number of nonlinear states under the repulsive interactions are similar to those presented in Ref.<sup>62</sup>.

2. Let  $V(x)$  be a double-well potential of finite depth (see Fig. 12C). Then, under certain restrictions, the solutions of Eq. (29) can be approximated by bound states composed of the solutions confined to each individual well. This statement is

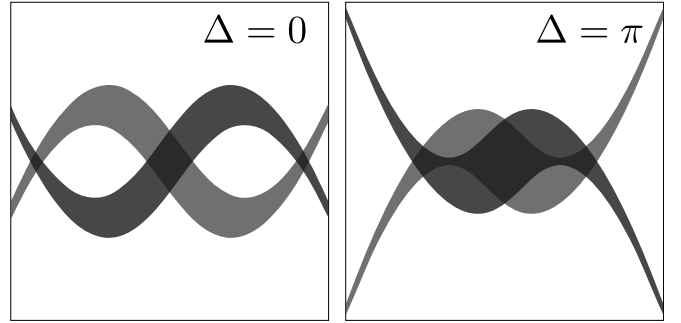


FIG. 10. Example 2: for  $\Delta = \pi$  island are not separated and the conditions of Hypothesis 1 are not satisfied. Each panel shows the region  $(u, u') \in [-2; 2] \times [-2; 2]$ .

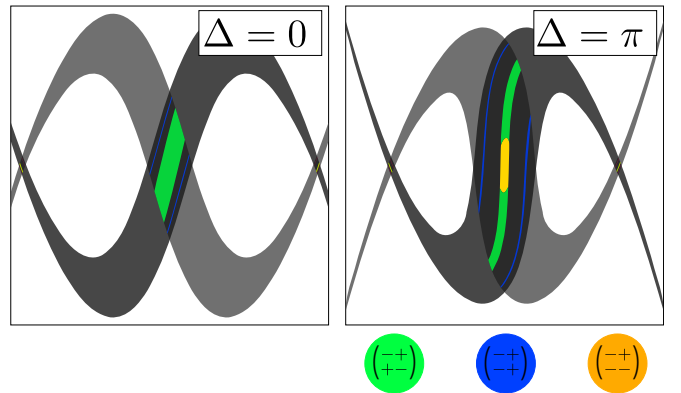


FIG. 11. Example 3: the signs of linearization matrices do not meet Theorem 2 conditions. Each panel shows the region  $(u, u') \in [-2.3; 2.3] \times [-2; 2]$ .

evident for well-separated potential wells but also holds when the wells are close.

3. Let  $V(x)$  be a periodic potential. It can be viewed as an infinite chain of identical, equally spaced wells of finite depth. The states localized within each elementary well can then serve as "building blocks" for constructing solutions of the full potential  $V(x)$ . This approach was employed in Refs.<sup>63,64</sup>, where the authors introduced a so-called "composition relation" linking the states defined on individual periods to solutions of the full equation. A rigorous justification for this treatment, in the form of a coding procedure, was provided in<sup>51,56</sup>. In these works, conditions were established that guarantee *any* combination of elementary cell states yields a valid nonlinear state of the periodic potential.

4. Now assume that  $V(x)$  is a quasiperiodic potential, which can be viewed as an infinite chain of finite depth potential wells. These wells are not fully identical and cannot be regarded as strictly equally spaced (see Fig. 9, gray line). From this viewpoint, the main result of the present paper consists in the conditions that guarantee the applicability of the "composition relation" for such a quasiperiodic — specifically, bichromatic — potential.

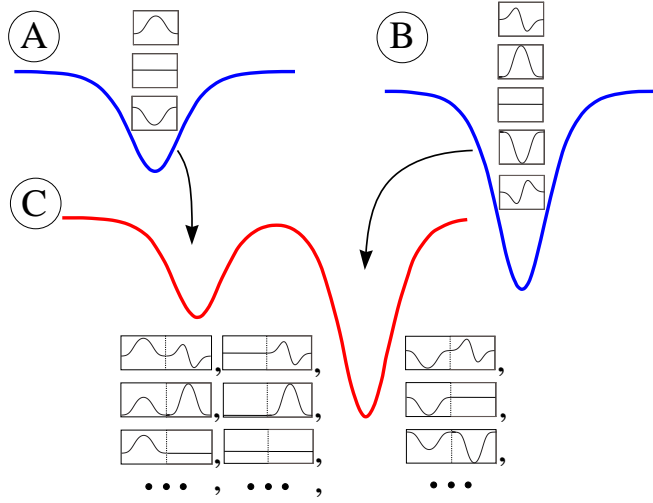


FIG. 12. Nonlinear states in a double-well potential (C), constructed as bound states of the individual well solutions (A and B).

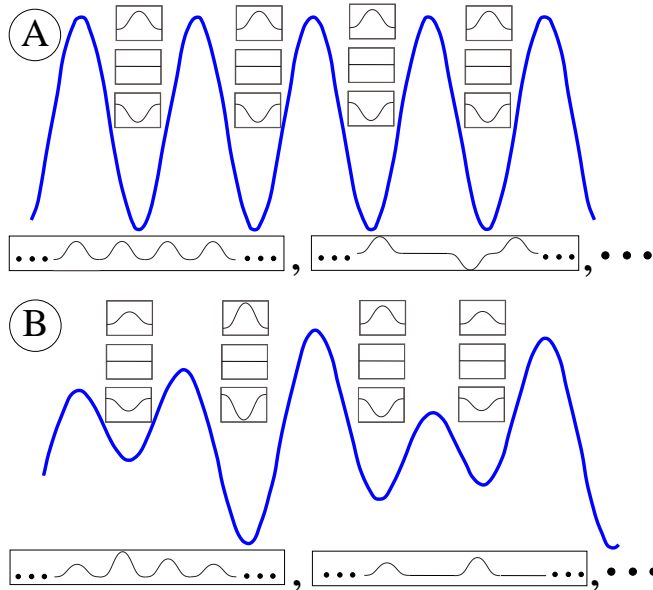


FIG. 13. Nonlinear states in (A) periodic and (B) quasiperiodic potentials, constructed as bound states of the individual well solutions.

### VIII. CONCLUSION

In this paper, we have developed a coding approach for stationary states of the one-dimensional Gross-Pitaevskii equation (GPE) with two incommensurate spatial frequencies. In the application to the theory of Bose-Einstein condensates, the incommensurate terms can originate from different physical mechanisms. The first mechanism is a superposition of two laser beams that form a quasiperiodic optical lattice. The second mechanism arises from a periodic modulation of the scattering length with a frequency that is incommensurate with that of the optical trap. The third possibility corresponds to the quasiperiodic scattering length.

We have demonstrated that, under certain conditions, the stationary states can be described using bi-infinite sequences of symbols from a finite alphabet. Our approach leverages the fact that, when the condensate is dominated by the repulsive interactions, a large subset of solutions to the Cauchy problem for the corresponding ordinary differential equation tend to infinity at some finite point on the real axis. The coding approach has been illustrated with a numerical example for the GPE with a quasiperiodic lattice.

Finally, we outline some problems amenable to the method developed in this work and suggest directions for its future development. A primary direction is the study of quasiperiodic versions of the GPE with a spatially modulated scattering length. This modulation could be periodic (with a frequency incommensurate with the optical trap) or quasiperiodic (resulting from the interplay of two incommensurate modulations). These studies should be followed by the analysis of stability of these nonlinear states keeping in mind possible relation between the codes of solutions and their stability.

The method can be further developed in several directions. First, it is promising to weaken the assumptions of Hypotheses 1 and 2. This may be achieved by considering the iterated maps  $\mathcal{P}^n$  and  $\mathcal{P}^{-n}$  for  $n \geq 2$  instead of  $\mathcal{P}$  and  $\mathcal{P}^{-1}$ . Numerical simulations suggest that using iterated maps leads to a contraction of the  $h$ - and  $v$ -strips, which could potentially extend the range of parameters for which the procedure is applicable. Second, in its current form, Theorems 2 and 3 are formulated in terms of the sign patterns of the entries of the Jacobian  $\mathcal{D}\mathcal{P}$ , which determine the mapping of quadrants. These theorems can likely be strengthened by considering arbitrary pairs of non-intersecting cones, rather than being restricted to quadrants. It would be valuable to extend the approach to cases with more complex nonlinearities and non-real-valued solutions.

A possible ramification of our approach could involve an application to Thouless pumping<sup>8,65</sup> of linear wave packets and solitons in periodic and quasiperiodic bichromatic lattices. In these studies (e.g., Refs.<sup>66,67</sup>), topological transport is achieved by adiabatically increasing the phase shift  $\Delta$  between the constituent sublattices. In the context of the present work, one topological pumping cycle would correspond to an adiabatic circuit around the donut as  $\Delta$  traverses the full space  $\mathbb{S}^1$ .

### ACKNOWLEDGMENT

The research of D.A.Z. was supported by Russian Science Foundation, Grant No. 25-12-00119, Ref.<sup>68</sup>.

### DATA AVAILABILITY

The data that supports the findings of this study are available from the corresponding author upon reasonable request.

<sup>1</sup>R. Lifshitz, What is a crystal? *Z. Kristallogr.* **222** 313317, (2007).

<sup>2</sup>R. Lifshitz, S. Schmid, R.L. Withers, *Aperiodic crystals* (Springer, 2013).

<sup>3</sup>D. Levine, P. J. Steinhardt, Quasicrystals: A New Class of Ordered Structures, *Phys. Rev. Lett.* **53**, 2477 (1984).

<sup>4</sup>D. Shechtman, I. Blech, D. Gratias, and J. W. Cahn, Metallic Phase with Long-Range Orientational Order and No Translational Symmetry, *Phys. Rev. Lett.* **53**, 1951 (1984).

<sup>5</sup>B. Freedman, G. Bartal, M. Segev, R. Lifshitz, D. N. Christodoulides, J. W. Fleischer, Wave and defect dynamics in nonlinear photonic quasicrystals, *Nature* **440**, 11661169 (2006).

<sup>6</sup>Y. Lahini, R. Pugatch, F. Pozzi, M. Sorel, R. Morandotti, N. Davidson, and Y. Silberberg, Observation of a Localization Transition in Quasiperiodic Photonic Lattices, *Phys. Rev. Lett.* **103**, 013901 (2009).

<sup>7</sup>P. Wang, Yu. Zheng, X. Chen, Ch. Huang, Ya. V. Kartashov, Ll. Torner, V. V. Konotop and F. Ye, Localization and delocalization of light in photonic moiré lattices, *Nature* **577**, 4246 (2020).

<sup>8</sup>O. Zilberberg, Topology in quasicrystals [Invited], *Opt. Mater. Express* **11**, 1143 (2021).

<sup>9</sup>J. E. Lye, L. Fallani, C. Fort, V. Guarrera, M. Modugno, D. S. Wiersma, and M. Inguscio, Effect of interactions on the localization of a Bose-Einstein condensate in a quasiperiodic lattice, *Phys. Rev. A* **75**, 061603(R) (2007).

<sup>10</sup>G. Roati, C. D'Errico, L. Fallani, M. Fattori, C. Fort, M. Zaccanti, G. Modugno, M. Modugno, and M. Inguscio, Anderson localization of a non-interacting BoseEinstein condensate, *Nature* **453**, 895898 (2008).

<sup>11</sup>J. B. Reeves, B. Gadway, T. Bergeman, I. Danahita, and D. Schneble, Superfluid Bloch dynamics in an incommensurate optical lattice, *New J. Phys.* **16**, 065011 (2014).

<sup>12</sup>H. P. Lüschen, S. Scherg, T. Kohlert, M. Schreiber, P. Bordia, X. Li, S. Das Sarma, and I. Bloch, Single-particle mobility edge in a one-dimensional quasiperiodic optical lattice, *Phys. Rev. Lett.* **120**, 160404 (2018).

<sup>13</sup>B. Deissler, M. Zaccanti, G. Roati, C. D'Errico, M. Fattori, M. Modugno, G. Modugno, and M. Inguscio, Delocalization of a disordered bosonic system by repulsive interactions, *Nat. Phys.* **6**, 354 (2010).

<sup>14</sup>G. Modugno, Anderson localization in BoseEinstein condensates, *Rep. Prog. Phys.* **73**, 102401 (2010).

<sup>15</sup>R. B. Diener, G. A. Georgakis, J. Zhong, M. Raizen, and Q. Niu, Transition between extended and localized states in one-dimensional incommensurate optical lattice, *Phys. Rev. A* **64**, 033416 (2001).

<sup>16</sup>S. K. Adhikari and L. Salasnich, Localization of a Bose-Einstein condensate in a bichromatic optical lattice, *Phys. Rev. A* **80**, 023606 (2009).

<sup>17</sup>J. Biddle, B. Wang, D. J. Priour, and S. Das Sarma, Localization in one-dimensional incommensurate lattices beyond the Aubry-André model, *Phys. Rev. A* **80**, 021603(R) (2009).

<sup>18</sup>M. Modugno, Exponential localization in one-dimensional quasiperiodic optical lattices, *New J. Phys.* **11**, 033023 (2009).

<sup>19</sup>D. J. Boers, B. Goedke, D. Hinrichs, and M. Holthaus, Mobility edges in bichromatic optical lattices, *Phys. Rev. A* **75**, 063404 (2007).

<sup>20</sup>Xiao Li, Xiaopeng Li and S. Das Sarma, Mobility edges in one-dimensional bichromatic incommensurate potentials, *Phys. Rev. B* **96**, 085119 (2017).

<sup>21</sup>H. Yao, H. Khoudli, L. Bresque, and L. Sanchez-Palencia, Critical Behavior and Fractality in Shallow One-Dimensional Quasiperiodic Potentials, *Phys. Rev. Lett.* **123**, 070405 (2019).

<sup>22</sup>T. Liu, X. Xia, S. Longhi and L. Sanchez-Palencia, Anomalous mobility edges in one-dimensional quasiperiodic models, *SciPost Phys.* **12**, 027 (2022).

<sup>23</sup>E. I. Dinaburg, Ya. G. Sinai, The one-dimensional Schrödinger equation with a quasiperiodic potential, *Funct. Anal. Appl.* **9**, 279289 (1975).

<sup>24</sup>O. Lesser, R. Lifshitz, Emergence of quasiperiodic Bloch wave functions in quasicrystals, *Phys. Rev. Res.* **4**, 013226 (2022).

<sup>25</sup>J. Moser, J. Pöschel, An extension of a result by Dinaburg and Sinai on quasi-periodic potentials, *Comment. Math. Helvetic* **59**, 39-85, (1984).

<sup>26</sup>J. Fröhlich, T. Spencer, and P. Wittwer, Localization for a Class of One Dimensional Quasi-Periodic Schrödinger Operators, *Commun. Math. Phys.* **132**, 5-25 (1990).

<sup>27</sup>S. Surace, Jr., The Schrödinger equation with a quasi-periodic potential, *Trans Amer. Math. Soc.* **320**, 321 (1990).

<sup>28</sup>L. H. Eliasson, Floquet Solutions for the 1-Dimensional Quasi-Periodic Schrödinger Equation, *Commun. Math. Phys.* **146**, 447-482 (1992).

<sup>29</sup>B. Simon, Almost Periodic Schrödinger Operators: A Review, *Adv. Appl. Math.* **3**, 463-490 (1982).

<sup>30</sup>Y. Last, Spectral theory of Sturm-Liouville operators on infinite intervals: a review of recent developments. In W.O. Amrein, A.M. Hinz, D.B. Pearson, *Sturm-Liouville theory: past and present*, pp. 99120 (Birkhauser, Basel, 2005).

<sup>31</sup>L. Pastur, A. Figotin, Spectra of random and almost-periodic operators, Springer-Verlag, Berlin (1992).

<sup>32</sup>L. P. Pitaevskii, BoseEinstein condensates in a laser radiation field, *Phys.-Usp.* **49**, 333351 (2006).

<sup>33</sup>V. A. Brazhnyi, V. V. Konotop, Theory of nonlinear matter waves in optical lattices, *Mod. Phys. Lett. B* **18**, 627651 (2004).

<sup>34</sup>O. Morsch, M. Oberthaler, Dynamics of BoseEinstein condensates in optical lattices, *Rev. Mod. Phys.* **78**, 179215 (2006).

<sup>35</sup>P. J. Y. Louis, E. A. Ostrovskaya, C. M. Savage, Yu. S. Kivshar, BoseEinstein condensates in optical lattices: band-gap structure and solitons, *Phys. Rev. A* **67**, 013602 (2003).

<sup>36</sup>G. L. Alfimov, V. V. Konotop, M. Salerno, Matter solitons in BoseEinstein Condensates with optical lattices, *Europhys. Lett.* **58**, 713 (2002).

<sup>37</sup>D. E. Pelinovsky, A. A. Sukhorukov, Yu. S. Kivshar, Bifurcations and stability of gap solitons in periodic potentials, *Phys. Rev. E* **70**, 036618 (2004).

<sup>38</sup>J. Yang, *Nonlinear Waves in Integrable and Nonintegrable Systems*, SIAM, Philadelphia, 2010.

<sup>39</sup>H. Sakaguchi, B. A. Malomed, Gap solitons in quasiperiodic optical lattices, *Phys. Rev. E* **74**, 026601 (2006).

<sup>40</sup>M. A. Porter, P. G. Kevrekidis, Bose-Einstein Condensates in Superlattices, *SIAM J. Appl. Dyn. Syst.* **4**, 783-807 (2005).

<sup>41</sup>Y. Kominis and K. Hizanidis, Power dependent soliton location and stability in complex photonic structures, *Opt. Express* **16**, 12124 (2008).

<sup>42</sup>C. Huang, C. Li, H. Deng, and L. Dong, Gap Solitons in Fractional Dimensions With a Quasi-Periodic Lattice, *Ann. Phys.* **531**, 1900056 (2019).

<sup>43</sup>H. C. Prates, D. A. Zezyulin, V. V. Konotop, Bose-Einstein condensates in quasiperiodic lattices: Bosonic Josephson junction, self-trapping, and multi-mode dynamics, *Phys. Rev. Res.* **4**, 033219 (2022).

<sup>44</sup>D. A. Zezyulin and G. L. Alfimov, Formation of nonlinear modes in one-dimensional quasiperiodic lattices with a mobility edge, *Phys. Rev. A* **110**, 063304 (2024).

<sup>45</sup>V. V. Konotop, Dimers and discrete breathers in Bose-Einstein condensates in a quasi-periodic potential, *Phys. Rev. Res.* **6**, 033113 (2024).

<sup>46</sup>Y. V. Kartashov, B. A. Malomed, and L. Torner, Solitons in Nonlinear Lattices, *Rev. Mod. Phys.* **83**, 247306 (2011).

<sup>47</sup>S. E. Pollack, D. Dries, M. Junker, Y. P. Chen, T. A. Corcovilos, and R. G. Hulet, Extreme Tunability of Interactions in a <sup>7</sup>Li Bose-Einstein Condensate, *Phys. Rev. Lett.* **102**, 090402 (2009).

<sup>48</sup>C. C. Chin, R. Grimm, P. Julienne, and E. Tiesinga, Feshbach resonances in ultracold gases, *Rev. Mod. Phys.* **82**, 1225 (2010).

<sup>49</sup>J. Zeng and B. A. Malomed, Two-dimensional solitons and vortices in media with incommensurate linear and nonlinear lattice potentials, *Phys. Scr.* **2012**, 014035 (2012).

<sup>50</sup>H. Sakaguchi, B. A. Malomed, Solitons in combined linear and nonlinear lattice potentials, *Phys. Rev. A* **81**, 013624 (2010).

<sup>51</sup>G. L. Alfimov, A. I. Avramenko, Coding of nonlinear states for the Gross-Pitaevskii equation with periodic potential, *Physica D* **254**, 29-45 (2013).

<sup>52</sup>G. L. Alfimov, P. P. Kizin, D. A. Zezyulin, Gap solitons for the repulsive Gross-Pitaevskii equation with periodic potential: Coding and method for computation, *Discrete Contin. Dyn. Syst. Ser. B* **22**, 1207-1229 (2017).

<sup>53</sup>G. L. Alfimov, P. P. Kizin, On solutions of Cauchy problem for equation  $u_{xx} + Q(x)u - P(u) = 0$  without singularities in a given interval, *Ufa Math. J.* **8**, 24-41 (2016).

<sup>54</sup>M. E. Lebedev, G. L. Alfimov, B. A. Malomed, Stable dipole solitons and soliton complexes in the nonlinear Schrödinger equation with periodically modulated nonlinearity, *Chaos* **26**, 073110 (2016).

<sup>55</sup>G. L. Alfimov, M. E. Lebedev, Complete description of bounded solutions for Duffing-type equation with periodic piecewise constant coefficient, *Rus. J. Nonlin. Dyn.* **19**, 473-506 (2023).

<sup>56</sup>M. E. Lebedev, G. L. Alfimov, Numerical Evidence of Hyperbolic Dynamics and Coding of Solutions for Duffing-Type Equations with Periodic Coefficients, *Regul. Chaotic Dyn.* **29**, 451473 (2024).

<sup>57</sup>G. L. Alfimov, M. E. Lebedev, On regular and singular solutions for equation  $u_{xx} + Q(x)u + P(x)u^3 = 0$ , *Ufa Math. J.* **2**, 3 (2015).

<sup>58</sup>N. Weaver, *Lipschitz algebras, Second Edition* (New Jersey, World Scientific, 2018).

<sup>59</sup>J. Moser, *Stable and random motion in dynamical systems* (Princeton University Press, Princeton, 1973).

<sup>60</sup>J. Guckenheimer, Ph. Holmes, *Nonlinear Oscillations, Dynamical Systems, and Bifurcations of Vector Fields* (Springer, 1983).

<sup>61</sup>S. Wiggins, *Introduction To Applied Nonlinear Dynamical Systems And Chaos* (Springer, 2003).

<sup>62</sup>G. L. Alfimov, D. A. Zezyulin, Nonlinear modes for the Gross–Pitaevskii equation — a demonstrative computation approach, *Nonlinearity* **20**, 2075 (2007).

<sup>63</sup>Yo. Zhang, B. Wu, Composition relation between gap solitons and Bloch waves in nonlinear periodic systems, *Phys. Rev. Lett.* **102**, 093905 (2009).

<sup>64</sup>Yo. Zhang, Zh. Liang, B. Wu, Gap solitons and Bloch waves in nonlinear periodic systems, *Phys. Rev. A* **80**, 063815 (2009).

<sup>65</sup>R. Citro and M. Aidelsburger, Thouless pumping and topology, *Nat. Rev. Phys.* **5**, 87 (2023).

<sup>66</sup>Q. Fu, P. Wang, Y. V. Kartashov, V. V. Konotop, and F. Ye, Nonlinear Thouless Pumping: Solitons and Transport Breakdown, *Phys. Rev. Lett.* **128**, 154101 (2022).

<sup>67</sup>X. Hu, Z. Li, A.-X. Chen, and X. Luo, Pumping of matter wave solitons in one-dimensional optical superlattices, *New J. Phys.* **26**, 123006 (2024).

<sup>68</sup><https://rsrf.ru/project/25-12-00119/>